MODELING AND FINANCIAL ANALYSIS OF A SOLAR-BIOMASS HYBRID POWER PLANT IN TURKEY

A THESIS SUBMITTED TO
THE GRADUATE SCHOOL OF NATURAL AND APPLIED SCIENCES
OF
MIDDLE EAST TECHNICAL UNIVERSITY

BY

MERVE ÖZDEMİR

IN PARTIAL FULFILLMENT OF THE REQUIREMENTS
FOR
THE DEGREE OF MASTER OF SCIENCE
IN
MECHANICAL ENGINEERING

SEPTEMBER 2017

Approval of the thesis:

MODELING AND FINANCIAL ANALYSIS OF A SOLAR-BIOMASS HYBRID POWER PLANT IN TURKEY

submitted by **MERVE ÖZDEMİR** in partial fulfillment of the requirements for the degree of **Master of Science in Mechanical Engineering Department, Middle East Technical University** by,

Prof. Dr. Gülbin Dural Ünver _____
Dean, Graduate School of **Natural and Applied Sciences**

Prof. Dr. R. Tuna Balkan _____
Head of Department, **Mechanical Engineering**

Assoc. Prof. Dr. Ahmet Yozgatlıgil _____
Supervisor, **Mechanical Engineering Dept., METU**

Examining Committee Members:

Assoc. Prof. Dr. Almıla Güvenç Yazıcıoğlu _____
Mechanical Engineering Dept., METU

Assoc. Prof. Dr. Ahmet Yozgatlıgil _____
Mechanical Engineering Dept., METU

Asst. Prof. Dr. Özgür Bayer _____
Mechanical Engineering Dept., METU

Asst. Prof. Dr. Feyza Kazanç _____
Mechanical Engineering Dept., METU

Prof. Dr. İskender Gökalp _____
ICARE, CNRS, France

Date: 05.09.2017

I hereby declare that all information in this document has been obtained and presented in accordance with academic rules and ethical conduct. I also declare that, as required by these rules and conduct, I have fully cited and referenced all material and results that are not original to this work.

Name, Last name: Merve ÖZDEMİR

Signature:

ABSTRACT

MODELING AND FINANCIAL ANALYSIS OF A SOLAR-BIOMASS HYBRID POWER PLANT IN TURKEY

Özdemir, Merve
MS, Department of Mechanical Engineering
Supervisor: Assoc. Prof. Dr. Ahmet YOZGATLIGİL

September 2017, 82 pages

Solar thermal and biomass combustion systems can be hybridized via a Rankine cycle to have a continuous electricity generation and lower CO_2 footprint. Disadvantages of these two renewable technologies can be overcome by hybridization. In this work; we develop a simulation model for Rankine cycle based, solar-biomass hybrid power plants using the ASPEN PLUS software. Solar parabolic collectors and biomass combustion are arranged in parallel to produce steam for power generation. Using the simulation model; thermal efficiency, fuel consumption rate, CO_2 emissions are investigated for 1 MW and 5 MW installed capacities. Besides, a financial analysis is conducted via MS EXCEL software. In the financial analysis, Net Present Value (NPV) and Internal Rate of Return (IRR) are calculated for both 1 MW and 5 MW installed capacities. According to the results, hybridization reduces biomass consumption by 18% and CO_2 emission by 20% compare to a stand-alone biomass power plant with the same installed capacity. IRR is calculated as 15.64% for 80% debt financing scenario.

Keywords: Solar-biomass hybrid, Concentrated Solar Power (CSP), Biomass Energy, Rankine Cycle

ÖZ

TÜRKİYE'DE BİR GÜNEŞ-BİYOKÜTLE HİBRİT SANTRALİNİN MODELLENMESİ VE FİNANSAL ANALİZİ

Özdemir, Merve
Yüksek Lisans, Makina Mühendisliği Bölümü
Tez Yöneticisi: Doç. Dr. Ahmet YOZGATLIGİL

Eylül 2017, 82 sayfa

Isıl güneş enerjisi sistemleri ve biyokütle yakma sistemleri kesintisiz elektrik üretimi ve daha düşük CO_2 ayak izi elde etmek için bir Rankine çevrimiyle hybridize edilebilir. Bu iki yenilenebilir teknolojinin dezavantajları hibridizasyon ile aşılabilir. Bu çalışmada, Rankine çevrimine dayalı güneş-biyokütle hibrit enerji santralinin simülasyon modeli Aspen Plus yazılımı kullanılarak yapılmaktadır. Elektrik üretiminde kullanılacak olan buharı elde etmek için parabolik oluklu güneş kollektörleri ve biyokütle kazanı paralel olarak kurulmuştur. Simülasyon modeli kullanılarak 1 MW ve 5 MW kurulu gücündeki sistemler için termal verim,yakıt tüketim oranları ve CO_2 emisyonları incelenmiştir. Bunun yanısıra, MS EXCEL yazılımı kullanılarak bir finansal analiz yapılmıştır. Finansal analizde, 1 MW ve 5 MW kurulu gücündeki sistemler için Net Bugünkü Değer ve İç Karlılık Oranı hesaplanmıştır. %80 borçlanma senaryosu için IRR %15.64 olarak hesaplanmıştır.

Anahtar Kelimeler: Güneş-Biyokütle Hibrit Santraller, Yoğunlaştırılmış Güneş Enerjisi, Biyokütle Enerjisi, Rankine Çevrimi

To my parents

ACKNOWLEDGMENTS

I would like to extend my sincere gratitude to my thesis supervisor, Assoc. Prof. Dr. Ahmet Yozgatlıgil for his great supervision, guidance and support throughout my graduate study. I feel grateful for all the time and effort he has spent on me, it is very much appreciated.

I would like to also extend special thanks to my co-advisor Dr. İskender Gökalp who gave me the opportunity to continue my study in the CNRS, France. I can say that it is not possible to finalize this study without his continuous and precious support.

My distinct thanks and gratitude go to my parents for their moral and material support and their patience throughout my life.

I would like to express my deepest gratitude to my dear friends Kadir Ali Gürsoy, Mahmut Murat Göçmen and Yiğitcan Güden for their extraordinary support that gives me the strength to continue in all circumstances.

I feel extremely privileged and proud for being a member of this study which is supported by the CNRS, the University of Orléans, the Excellency Center LABEX CAPRYSSES and METU.

TABLE OF CONTENTS

LIST OF TABLES

TABLES

LIST OF FIGURES

FIGURES

NOMENCLATURE

BFB	Bubbling Fluidized Bed
CAPEX	Capital Expenditures
CFB	Circulating Fluidized Bed
CHP	Combined Heat and Power
CPI	Consumer Price Index
CSP	Concentrated Solar Power
DNI	Direct Normal Irradiance
DSG	Direct Steam Generation
FC	Fixed Carbon
HTF	Heat Transfer Fluid
IRR	Internal Rate of Return
LCOE	Levelized Cost of Electricity
LFR	Linear Fresnel Reflector
$M_{b\text{-}water}$	Mass flow rate of the water in the biomass boiler
$M_{biomass}$	Mass flow rate of the biomass
$M_{methane}$	Mass flow rate of methane
M_{oil}	Mass flow rate of the heat transfer fluid
$M_{s\text{-}water}$	Mass flow rate of the water in the solar field
MW_e	Megawatt electrical
MW_{th}	Megawatt thermal
$\eta_{thermal}$	Thermal Efficiency
NPV	Net Present Value
O&M	Operation and Maintenance
OPEX	Operational Expenditures
PDC	Parabolic Dish Collector
PTC	Parabolic Trough Collector
PV	Photovoltaic
$q_{biomass}$	Heat Input from Biomass Boiler
Q_{in}	Heat transfer to the heat transfer fluid

q_{solar}	Heat Input from Solar Collectors
SPT	Solar Power Tower
VM	Volatile Matter
w_{pump}	Pump Work
$w_{turbine}$	Turbine Work

CHAPTER 1

INTRODUCTION

Global electricity consumption increases as the population grows and technology develops. According to the statistics, world electricity consumption has increased by 30% in the last 10 years [1].

Most of the electricity generated in the power plants comes from thermal sources which are based mainly on fossil fuels. Therefore, an increment in electricity demand causes more consumption of fossil fuels which rises CO_2 emissions. Moreover, the amount of available fossil resources will not be enough to meet the growing electricity demand since they are exhaustible.

The limited supply of fossil hydrocarbon resources and the negative impact of CO_2 emissions on the global environment dictate efficient use of energy and renewable energy applications.

Turkey has substantial amount of renewable energy potential and the utilization rates are growing. The total installed capacity is 80.3 GW as of June, 2017 and 20.1% of it are based on renewable energy sources [2]. The government targets to reach renewable installed capacities of 5,000 MW solar, 1,000 MW biomass, 1,000 MW geothermal, and 20,000 MW wind power by 2023 and within this approach Turkey's Renewable Energy Support Mechanism is formed.

One of the topics covered by the Support Mechanism is the Feed-in-Tariff policy which sets a fixed, guaranteed price over a stated fixed-term period at which small or large generators can sell renewable power to the electricity network. According to Law No.5346, power plants that have come into operation since 18 May 2005 or will come into operation before 31 December 2020 will be eligible to receive the feed-in-tariffs shown in Table 1 for the first ten years of their operation [3].

Depending on the renewable resource, bonus to feed-in-tariffs shall be added to the existing tariff in case locally manufactured electromechanical equipment is used in generating facilities. This additional tariff is valid for 5 years from the commercial operation date. In addition to feed-in-tariff policy, renewable energy based electricity generation facilities developed by the real persons and legal entities up to 1 MW installed capacity is free of license.

Table 1 Feed-in-Tariff Mechanism [3]

Type of Power Plant Facility	**Price**	**Max. Local Production Premium**	**Max. Possible Tariff**
Hydroelectric	$7.3 cents / kWh	$2.3 cents/kWh	$9.6 cents/kWh
Wind	$7.3 cents / kWh	$3.7 cents/kWh	$11 cents/kWh
Geothermal	$10.5 cents / kWh	$2.7 cents/kWh	$13.2 cents/kWh
Biomass	$13.3 cents / kWh	$5.6 cents/kWh	$18.9 cents/kWh
Solar PV	$13.3 cents / kWh	$6.7 cents/kWh	$20 cents/kWh
Concentrating Solar	$13.3 cents / kWh	$9.2 cents/kWh	$22.5 cents/kWh

With the rapidly growing unlicensed market, both Photovoltaic (PV) and Concentrated Solar Power (CSP) capacities in Turkey are expected to reach a competitive level in a very short period. For example a 5 MW solar power tower is constructed with 500 heliostats in Mersin [4]. 1,363 MW of photovoltaic solar power plant is under operation since June, 2017 [5]

Figure 1 Installed CSP System in Mersin [4]

In terms of availability, solar energy is among the most abundant renewable energy type in Turkey. Figure 2 shows the Global Solar Radiation map of Turkey [6].

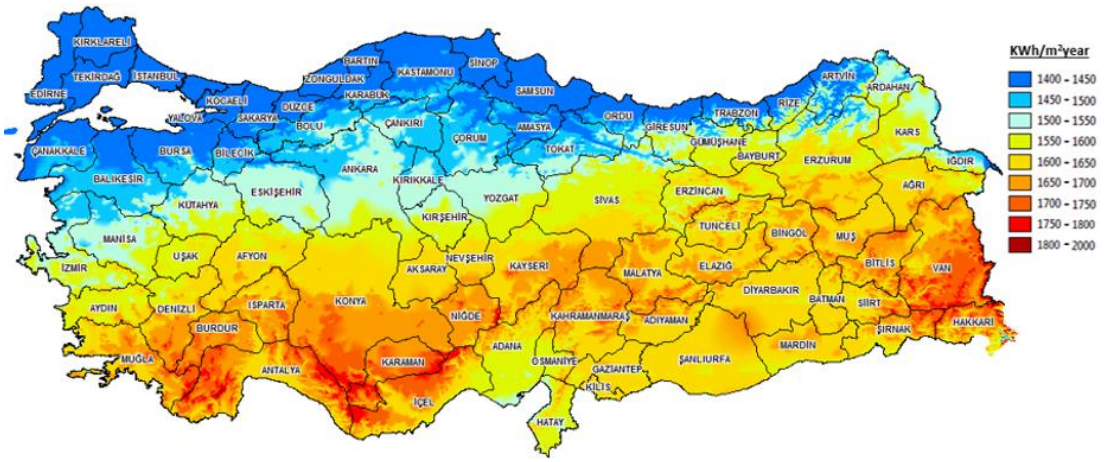

Figure 2 Solar Map of Turkey (kWh/m^2 year) [6]

As can be seen from the figure, in most of the regions the global solar radiation is above 1500 kWh/m^2/year and especially in southern regions, values even higher than 1800 kWh/m^2/year can be observed.

There are 78 licensed biomass power plants in Turkey with 398 MW installed capacity and 267 MW among them is under operation. Biomass means organic matter like forest

residues (branches, dead trees, and tree stamps), wood chips, yard clippings, and municipal solid waste. Landfill gas energy generation plants are also developing in Turkey. Several investors are getting through a tender process managed by municipalities to sell their waste in the city dump area for waste to energy developers. Besides, forest based biomass energy potential of Turkey, as can be seen from Figure 3, is also high.

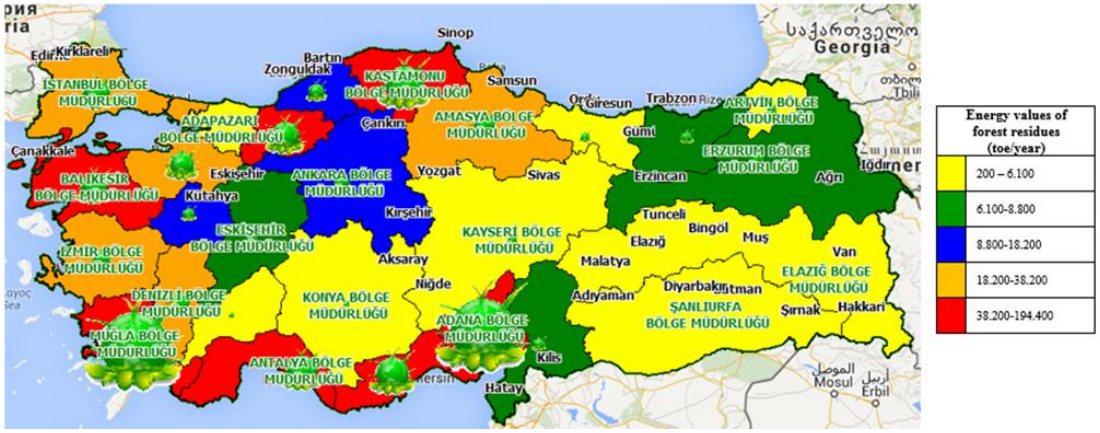

Figure 3 Forest Based Biomass Potential of Turkey (toe/year) [7]

According to the current installed capacity breakdown of Turkey, it is seen that the contribution of solar and biomass energy to the renewable energy installed capacity is around 1% for each resource. This percentage is quite low when we consider the solar and biomass energy potential of Turkey. Considering the Support Mechanism and the current installed capacity in Turkey, there are plenty of room to go further especially in terms of solar and biomass energies.

Solar energy is inexhaustible and no fuel cost is required for electricity generation. However, because of the dependence on sunshine hours, stand-alone solar power plants do not produce energy for an important portion of time during the year. It is the biggest disadvantage of solar energy because electricity is also demanded during night time. Adding a thermal storage system is one solution to solve this intermittency problem. On the other hand, electricity storage technologies are quite expensive to install them with a sufficient size.

In terms of biomass energy, it is possible to obtain continuous electricity generation. Power plants based on biomass energy can provide base load if there is sufficient

amount of biomass fuel in their feed stock. Seasonal fluctuations of the available source are another problem. Therefore, biomass plants need large storage areas to secure their production. Moreover, transporting biomass from where it is harvested to the power plant location requires a complex logistics system and increases the fuel cost of power plants based biomass energy.

In order to have a reliable and sustainable solution for meeting the increasing electricity demand, one should minimize the disadvantages of aforementioned resources. Combining solar energy and biomass energy is a suitable method to obtain continuous energy production. Compared to other renewables, biomass energy has a more predictable nature and hybridizing solar energy with biomass energy is a promising solution to overcome their individual disadvantages.

The most common method for the hybridization of solar and biomass energy to produce electricity is the Rankine cycle. There are several techniques in which solar and biomass energy are used to produce process steam for Rankine cycle. Concentrated Solar Power technology is used to convert solar energy into thermal energy which can be utilized in the Rankine cycle. Combustion technologies are suitable to obtain heat from biomass energy to generate steam.

The following section explains the concentrated solar power and biomass conversion technologies in detail.

1.1 Concentrated Solar Power (CSP) Technologies

CSP Technologies redirect and focus direct sunlight onto a small area where the solar energy is converted into thermal energy. CSP systems can only use direct solar radiation which reaches the Earth's surface as parallel beam and called Direct Normal Irradiance (DNI) [8].

There are four main types of CSP Technologies; (1) Parabolic trough collectors (PTCs), (2) Linear Fresnel Reflectors (LFRs), (3) Parabolic Dish Collectors (PDCs) and (4) Solar Power Towers (SPTs). According to their focus geometry, the systems can be divided into two groups as point focus collectors (PDCs and SPTs) and line focus collectors (PTCs and LFRs)[9].

1.1.1 Parabolic Trough Collectors (PTCs)

The parabolic trough collector system basically consists of a reflective material (mirrors), a receiver pipe (absorber tube), tracking system and metal construction to support the collector[10]. A sheet of reflective materials bent into parabolic shape and put together in series to form long troughs. These parabolic shaped mirrors have a linear focus along which a receiver pipe is mounted. Sun radiation is redirected and concentrated towards absorber tube and transformed into thermal energy. The heat transfer fluid (HTF) circulates through the receiver tube, collecting and transporting thermal energy. Currently, synthetic oil, water and molten salts are the heat transfer fluids used in parabolic trough collectors [10]. Due to its low volatility and higher boiling point, oil is generally chosen as HTF in commercial plants. However, the maximum working temperature of oil is around 400°C and it limits the efficiency [11]. Hazardous effect of toxic and flammable synthetic oils to the environment is another drawback. When water is utilized, evaporation of water takes place in the absorber tube and the configuration is called direct steam generation (DSG). In parallel-trough systems using DSG, higher steam temperature and absence of heat exchangers increase the efficiency. On the other hand, water applies more stress on the absorber tubes because of its relatively high volatility [10]. Corrosion problem in tubes and control difficulty of two-phase flow are the disadvantages of DSG.

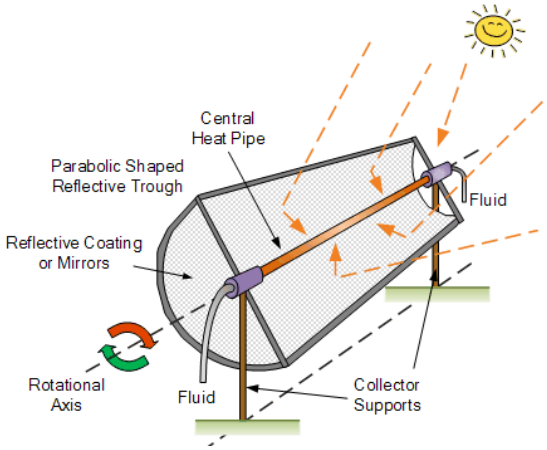

Figure 4 Schematic Diagram of PTC System [12]

1.1.2 Linear Fresnel Reflectors (LFRs)

Operating principle of Linear Fresnel Reflectors is very similar to PTCs. Instead of a curved reflector, ground mounted flat plate mirrors focus the irradiation onto the absorber tube which is fixed over them. The receiver pipe is mounted over a tower above and along the linear reflectors. Since the reflectors are mounted close to the ground, structural requirement is minimized. Besides, flat mirrors are cheaper than parabolic reflectors.

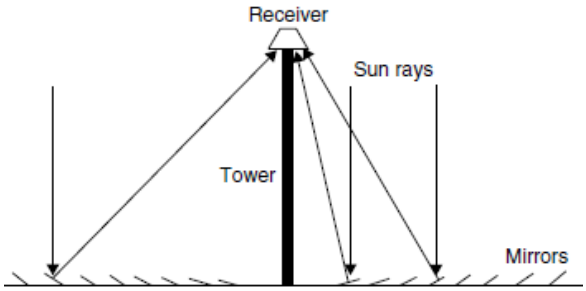

Figure 5 Schematic Diagram of LFR System [11]

1.1.3 Parabolic Dish Collectors (PDCs)

Parabolic Dish Collector is a point focus collector which consists of a parabola shaped reflector and a receiver mounted at the focus of the parabola [10]. Concentrating ratio of the dish systems is very high so that they can achieve temperatures in excess of 1500°C [11]. In addition, PDCs have the highest transformation efficiency among other CSP systems. Parabolic dish collectors are very large mirrors and they must have almost perfect concavity to efficiently concentrate solar radiation [10]. For that reason, their costs are very high and it is the most important disadvantage of PDCs.

1.1.4 Solar Power Towers (SPTs)

A field of distributed mirrors called heliostats are used as reflectors in Solar Power Towers. Heliostats consist of several flat mirrors and focus the sunlight to a central receiver mounted on the top of a tower [10]. A heat transfer fluid passing through the central receiver absorbs the solar energy and generate steam to power a conventional turbine. Since the heliostats focus large amount of solar radiation into a small area, heat losses are minimized and high concentration ratios are achieved. SPTs can thus

operate at very high temperatures [11]. Comparing to other CSPs, SPTs require the biggest area per unit of generated energy and large quantity of water [13].

1.2 Biomass Conversion Technologies

Thermochemical conversion processes allow to produce heat and electricity or combined heat and power (CHP) from biomass. Direct Combustion, Gasification and Pyrolysis are the common types of this method.

1.2.1 Direct Combustion

Direct combustion of the fuel is the simplest way of biomass conversion. In the combustion process, biomass burns with air and produces ash and hot gases at temperatures around 800–1000°C [14]. Chemical energy in the biomass transforms into thermal energy which is available in the form of hot flue gases. The quantity of thermal energy is generally defined by the calorific value of burned biomass. It is possible to burn any type of biomass however, combustion is feasible only for biomass with a moisture content below 50% [14]. For higher moisture content, biomass must be dried before feeding to the furnace. Combustion takes place in the furnace and the resultant thermal energy is transferred to another medium in the boiler. In most applications boiler and furnace are closely integrated [15].

Combustion technologies for biomass can be grouped as “Fixed Bed” and “Fluidized Bed” Systems. Fix Bed Systems include grate furnace and underfeed stoker [16]. Whereas Fluidized Bed Systems contain bubbling fluidized bed (BFB) and circulating fluidized bed (CFB) [15]. In fixed bed systems, primary air is supplied through a fixed bed where the combustion takes place. Ash removal system of grate furnaces are more efficient than that of under-stoker furnaces, so under-stoker furnaces are not suitable also for high ash content fuels.

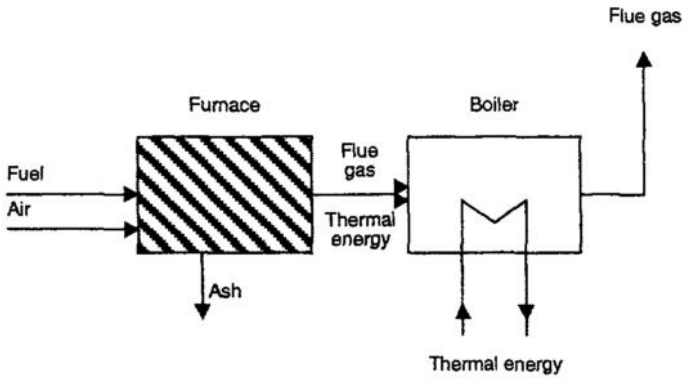

Figure 6 Basic Process Flow for Biomass Combustion [15]

There are several types of grate furnaces such as fixed grates, moving grates, travelling grates, rotating and vibrating grates [16]. Schematic diagram of a grate furnace is shown in Figure 7. Biomass is fed at the top and moves downward during the combustion process and the ash is removed at the bottom.

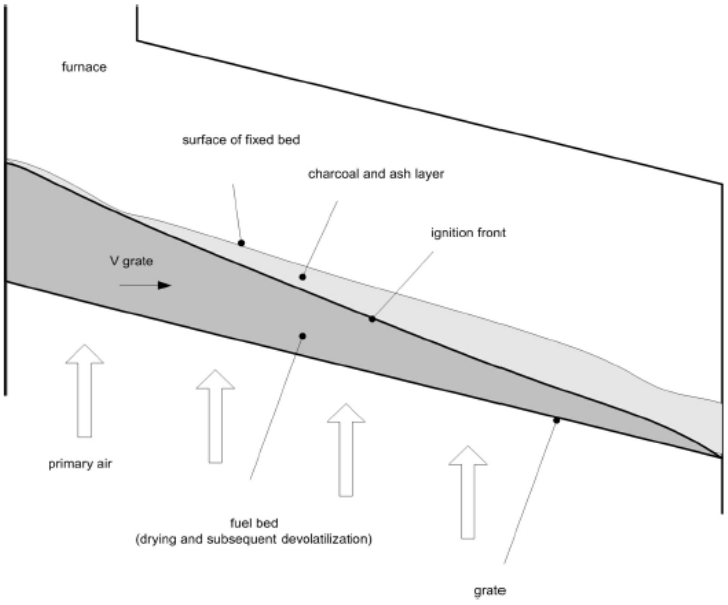

Figure 7 Schematic Diagram of Grate Furnace [16]

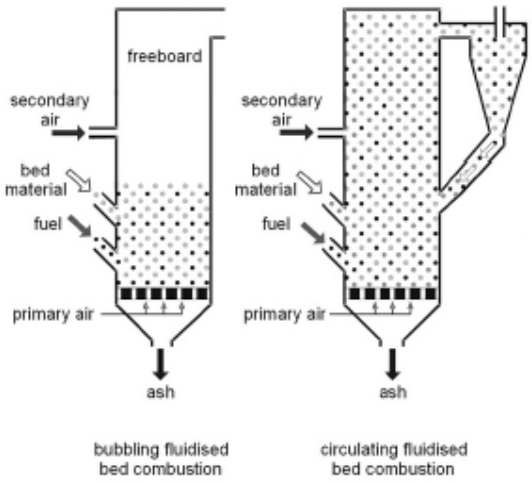

Figure 8 Schematic Diagram of Fluidized Bed Combustion Systems [16]

In fluidized bed combustion system, primary air enters from below and biomass is burned in a hot inert and granular material that is kept in turbulent suspension with fans [16]. Depending on the air velocity, they can be classified as bubbling and circulating beds. Circulating fluidized beds require smaller particles and a higher fluidizing velocity.

Biomass having high moisture (up to 60%) and ash (up to 50%) content can be burned using fluidized bed furnaces [15]. Combustion efficiency is higher and the flue gas flow is lower compare to fixed bed system however, their investment costs are relatively high. Therefore, fluidized bed systems are more feasible for large scale plants (larger than 30 MW_{th}) [16].

1.2.2 Gasification

Gasification of biomass can be defined as the conversion process in which a combustible gas is produced by partial oxidation of solid biomass at high temperatures [14]. The gas can be further converted to produce chemicals or burned directly to obtain thermal energy [14], [17].

It is possible to use air or pure oxygen as the gasifying medium. In the case of pure oxygen, the resultant gas has a higher energy content but the cost is also higher compare to air gasification [18].

1.2.3 Pyrolysis

Pyrolysis is the thermochemical conversion process that allows to produce liquid, solid and gas fuel by heating the biomass in the absence of air [19]. The gas mainly includes hydrogen, carbon monoxide, carbon dioxide, methane. The liquid components are methanol, acetic acid, acetone, water and tar whereas the solid residue consists of carbon and ash [18].

1.3 Objectives of the Thesis

The main objective of this thesis is to analyze the economic feasibility, biomass consumption and CO_2 emissions of a solar-biomass hybrid power plant in Turkey. Within this scope, a simulation model is developed to numerically simulate this power plant and investigate the annual biomass consumption and CO_2 emission amounts of this system. Moreover, a financial model is developed to examine the economic feasibility of the project with regards to the overall gain through its operational life.

In order to make a comprehensive research, two different installed capacities (1 MW_e and 5 MW_e) for the power plant are analyzed. These capacities are selected due to economic concerns. According to the current legislation in Turkey, 1 MW_e is the legal limit to build and operate a power plant without demanding an electricity generation license. Obtaining the license requires to complete a list of bureaucratic processes which cost time and increase the initial expenditures. Biomass amount is another constraint for the size of the installed capacity. When the installed capacity of operating biomass power plants in Turkey is examined, the average installed capacity is around 5 MW which is based on the available annual biomass amount to operate the plant continuously. Another selection is made for the location of the plant. Solar energy and biomass energy potential is considered for the selection. Kırklareli is preferred since the forest based biomass potential of the region is high which minimizes the transportation costs and the logistic problem. Moreover, if a power plant in Kırklareli is found feasible, power plants located in other regions which have a higher solar energy potential compare to Kırklareli will be found feasible without doubt.

In the following sections, Chapter 2 presents the current concepts which are available in the literature. Chapter 3 gives the information regarding the simulation model. The

technical details about the design and the results obtained from this model are presented in Chapter 4. The financial model together with its assumptions, inputs and results are explained in Chapter 5. Finally, Chapter 6 summarizes the main results and presents some future works.

CHAPTER 2

LITERATURE SURVEY

2.1 Current Solar Hybrid Power Plant Studies in Turkey

Regarding hybridization of solar power with other renewable and conventional energy sources in Turkey, there are not much more studies. In 2012 Yılmazoğlu et al. investigated solar repowering of the Soma-A Thermal Power Plant (TPP) in Manisa, Turkey for full load and part load operations. Current situation of the power plant has been compared with two solar repowering cases which are Case-B (superheating the feed water heater before the steam turbine) and Case-C (replacing all feed water heaters by solar collectors) shown in Figure 9. Certain fraction of steam is generated by parabolic trough collectors as a result CO_2 emission per kWh decrease 14% at full load operations. Whereas, at part load operations, the TPP generates 14% more electricity using same amount of fuel [20].

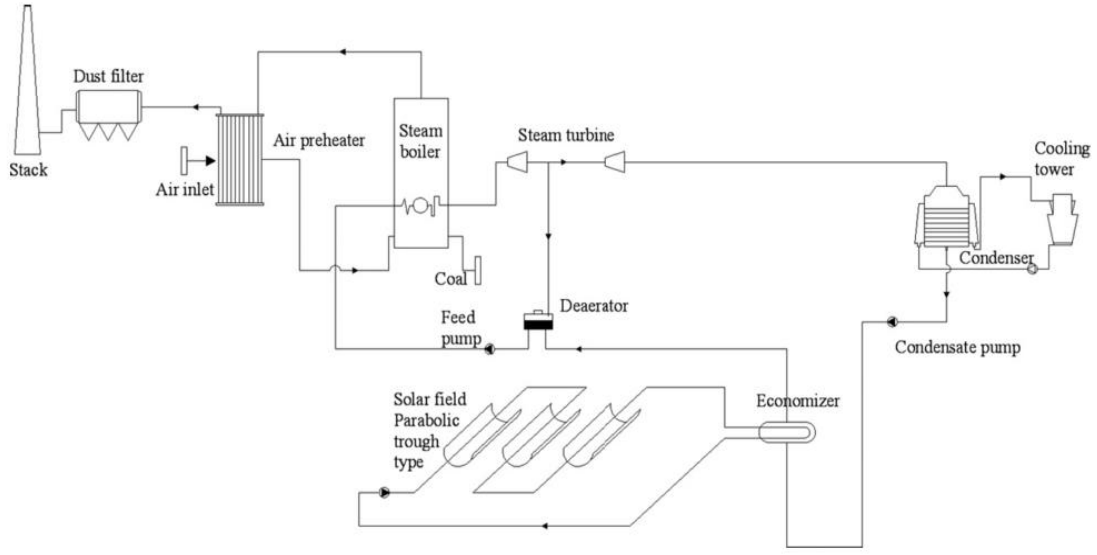

Figure 9 Schematic Diagram of Solar Repowering of Soma-A TPP / Case-C [20]

The first Geothermal-CSP Hybrid Power Plant (Gümüşköy GPP) over world has been commissioned in April 2014 in Aydın, Turkey [21]. Gümüşköy GPP, which has binary

cycle technology with an installed capacity of 10.2 MW_e, is developed by BM Holding and the investment cost of the project is around $ 50 M. Air-cooled condensers are utilized in the system and the plant suffers a decrease in power produced during hot seasons due to high ambient temperature. The increase in ambient temperature causes loss of overall efficiency up to 40% and the net power capacity could drop to as low as 7.3 MW_e for several months. In order to overcome this problem, a hybrid concept in which the geothermal fluid is heated by solar collectors before it enters the turbine is designed. Kuyumcu et al. evaluated the effect of solar collectors on power plant efficiency and electricity generation[22]. Site application of the concept is performed by TYT Engineering. Installed thermal power of the PTC system is 200 kW and generates 330,000 kWh thermal power per year which corresponds to a saving of 60.8 ton CO_2 [21]. Figure 10 shows the cycle diagram for solar-geothermal hybrid power plant.

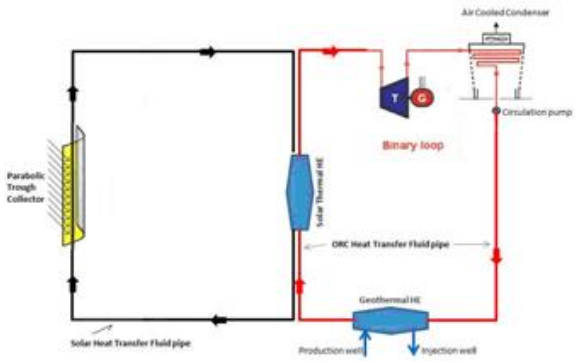

Figure 10 Gümüşköy Hybrid GPP Cycle Diagram[22]

Another assessment regarding the solar-geothermal hybrid power plant potential in Menderes Graben, Turkey is conducted by Turan in 2015[23]. The study focuses on combining the low enthalpy geothermal systems based on Organic Rankine Cycle (ORC) with PTCs for superheating binary cycle fluids to higher temperatures thereby increasing their enthalpy for more feasible energy conversion.

Solmaz et al. performed a feasibility study for 500 kW solar-wind hybrid power plant installed in Gediz University Campus, İzmir in 2015[24], [25]. The wind turbine power is 100 kW and capacity factor is 13% which results 112.054 kWh electricity generation per year. The power plant can save 450 ton CO_2 per year.

2.2 Studies on Solar-Biomass Hybrid Power Plants

2.2.1 Operating Solar-Biomass Hybrid Plants

Termosolar Borges is the first commercial CSP plant hybridized with biomass and it has 22.5 MWe installed capacity.[26]. The power plant was constructed in the North East of Spain with 1812 kWh/m^2/year direct irradiation[26]. Parabolic trough technology is used in the solar part. The received solar irradiation in the solar field based on 336 collectors (56 parallel loops of 6 parabolic trough collectors) with a total area of 181,000 sqm from the installed mirrors[26]. Each collector has a system of parabolic reflectors that concentrate the solar radiation on the heat collecting element where solar energy is transferred to heat transfer fluid (HTF).

Hybrid system has two biomass boiler, each producing approximately 22 MW_{th} and have 10 MW natural gas burners can use biomass or natural gas as a fuel depending on the meteorological conditions [27]. Another 6 MW heater operates exclusively on natural gas, and such the installed combustion thermal capacity does not exceed 50 MW_{th} [27].

The plant can operate in three modes, (1) Solar Mode (2) Mixed Mode (3) Biomass Mode alone allowing the turbine to operate at 50% of its maximum load. Electrical efficiency from the turbine at full load is 37%. The power block has a single shaft steam generator. The solar field generates saturated steam at 40 bar and the biomass boilers superheat this steam to 520 °C[26]. Thermosolar Borges generates 98,000 MWh electric power annually with an operation time of 5.400 h/year for biomass part and nearly 1000 h/year for solar part, 6400 h/year in total and saves 24,500 ton CO_2 per year[26].

Morel compared CSP-biomass hybrid system generating same amount of electricity with a PV plant at the same location. The study shows that hybrid system unit generation per installed power is 3.4 times greater than the generation of PV plant. The investment cost for hybrid system is 22% higher that the PV plant. Besides, the required surface area for hybrid system is nearly half of that required for PV plant.

The biomass input is approximately 66,000 tons per year at 45% humidity and mainly consists of forest residue and agricultural crops[27].

Rende Hybrid Plant is another hybrid solar-biomass power plant located in Calabria, southern Italy. In this project, an existing 14 MWe biomass plant is converted into a 15 MWe hybrid biomass-CSP plant by integrating a 1 MWe Fresnel type CSP component [28]. As a result of hybridization, the efficiency of the existing system is increased.

Desai et al. developed a simulation to optimize the operating features of a 1 MW solar thermal power plant commissioned in New Delhi, India in 2013. The plant has two different solar fields (PTCs and LFRs) connected to a single turbine operated by steam at 350°C, 42 bar. Therminol VP-1 is used as HTF in PTCs whereas Direct Steam Generation (DSG) is preferred in LRFs. Process flow diagram of the power plant is shown in Figure 11. Annual DNI at New Delhi is 1273 kWh/m^2-year and the power plant generates 1365 MWh electricity per year at a capacity factor of 15.6% [30]. There are no fossil fuel or biomass based auxiliary heater in the plant.

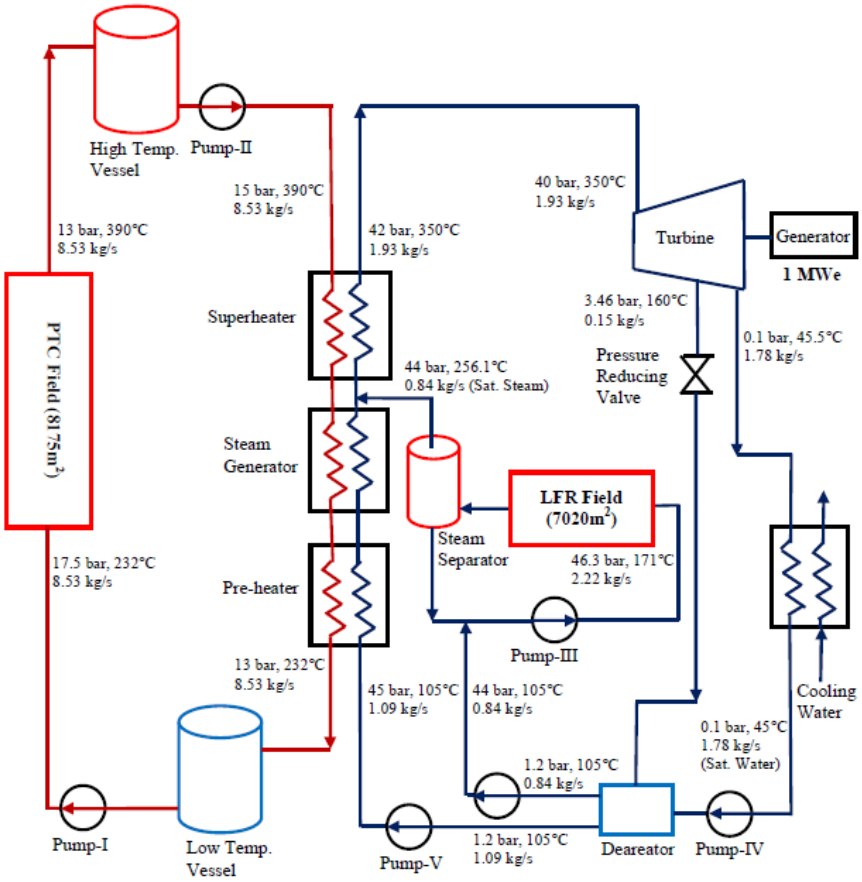

Figure 11 Process Flow Diagram of 1 MW Power Plant in New Delhi, India [30]

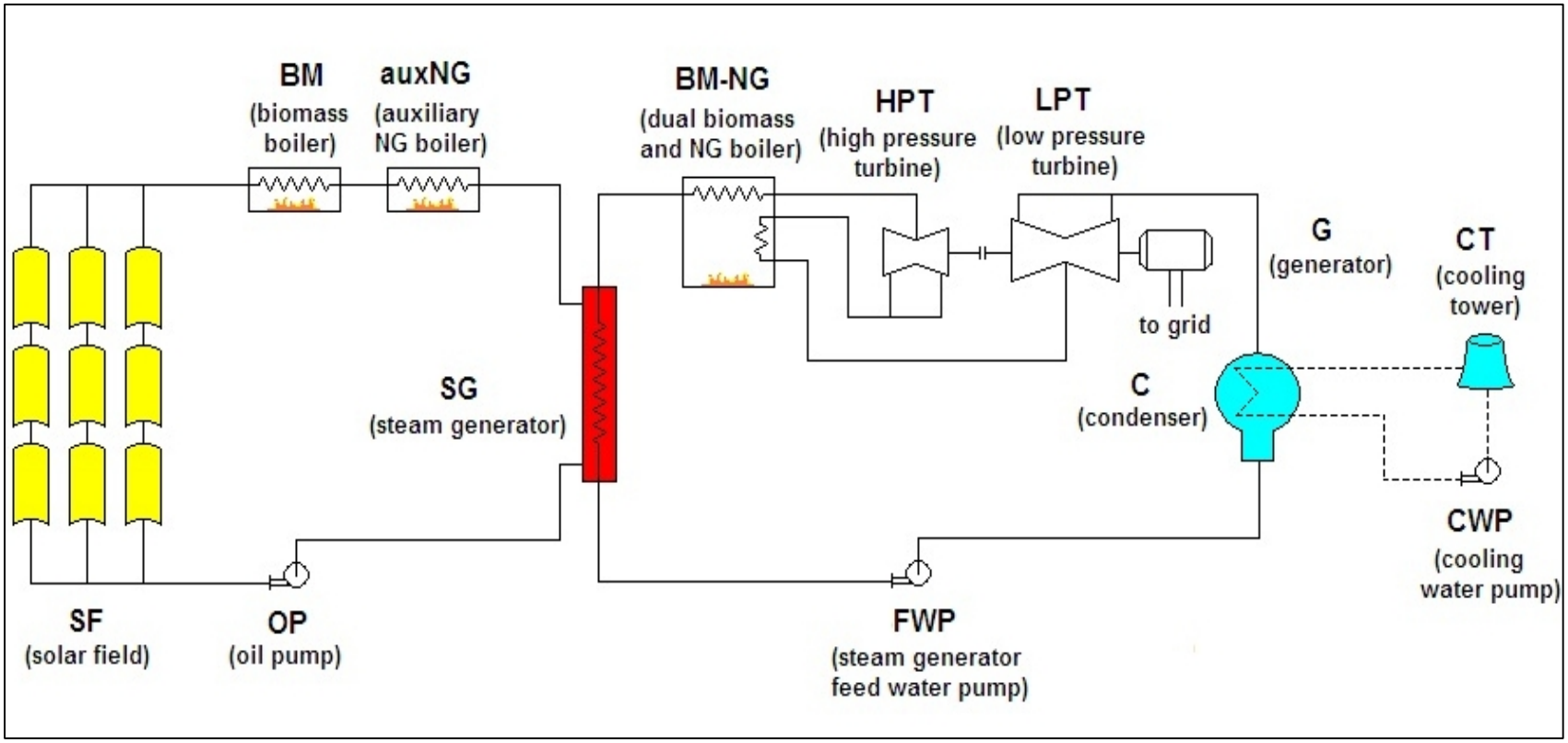

Figure 12 Schematic of Termosolar Borges [29]

As a result, the inherent variation and discontinuity in the output of solar fields, such as cloud cover may cause disruptions in smooth running of the turbine and also can cause shutdowns in winter season. The turbine can operate up to 250 kW and the simulation results also show that the plant is nearly not able to operate due to low DNI values in January, July, August and December. On the other hand, maximum output is obtained in April (232 MWh) and May where the DNI values are comparably high.

2.2.2 Theoretical Studies on Solar-Biomass Hybrid Power Plants

Performance characteristics of solar-biomass hybrid power plant without energy storage is examined by Srinivas et al[31]. The said plant is operated on a simple regenerative Rankine cycle, shown in Figure 13, and the steam is generated from both solar and biomass systems.

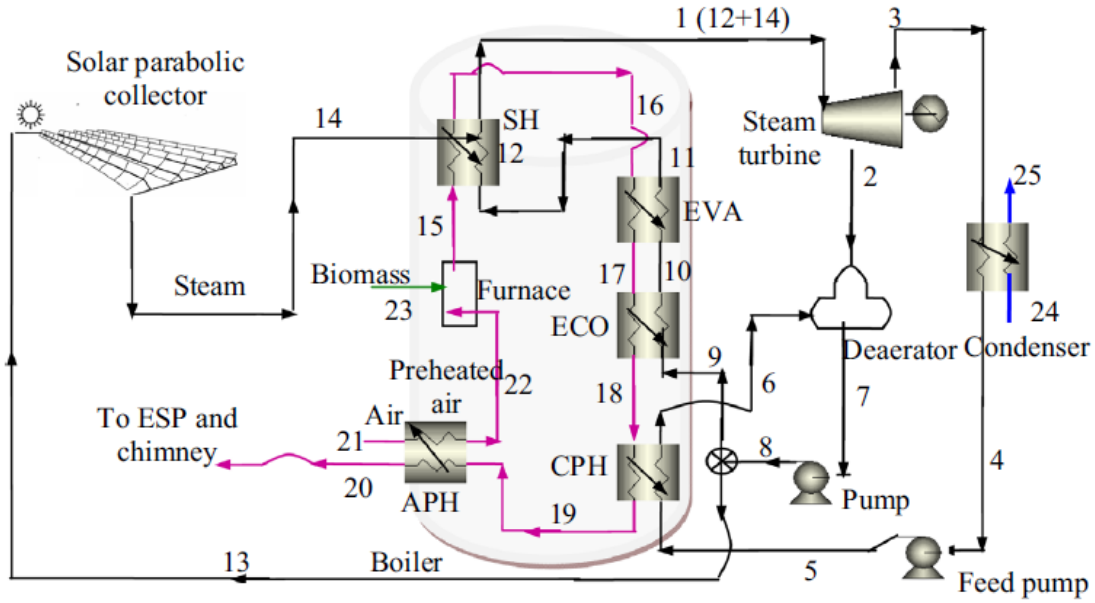

Figure 13 Flow Diagram of Solar-Biomass Hybrid Power Plant used in Srinivas's Study[31]

In that work, thermal efficiency of the cycle, thermal efficiency of the hybrid plant, plant fuel efficiency and specific power are investigated under variable solar radiation and turbine inlet conditions. The effect of pressure variation from 20 bar to 60 bar and steam temperature from 300°C to 450°C on performance characteristics is investigated. At 20 bar boiler pressure, a change in solar share from 10% to 50% increases the plant fuel energy efficiency from 16% to 29%. It is found that the thermal

efficiency of the hybrid plant decreases as the steam temperature in boiler increases. On the other hand, it increases with increasing boiler pressure. An increase in boiler pressure (10-60 bar) and turbine inlet temperature (300-450°C) vary the specific power and cycle thermal efficiency as 0.62-0.82 kW/kg steam and 24-29% respectively.

Feasibility of solar-biomass hybrid power plants for various applications with an installed capacity ranging from 2 to 10 MW thermal power is assessed in terms of technical, financial and environmental criteria by Nixon et al. Assessment is based on five case studies and a simulation model is developed in that regard. Results are compared with standalone biomass fired power plants and it is found that 29% of biomass saving is achieved by hybrid operation [32], [33].

Servert et al. analyzed CSP-biomass hybrid plants and exercised different configurations for 10 MW installed power. The configuration in which solar and biomass systems are connected in parallel and able to generate electricity separately shown in Figure 14. A comparison between hybrid system, conventional standalone CSP and biomass power plant has been performed. The study shows that investment cost of hybrid systems is 24% lower than a simple addition of investment costs of two standalone power plants since some of the equipment is shared by both CSP and biomass systems. Besides, effective operating hours and overall energy generation of hybrid power plant is 2.77 times higher than the conventional CSP systems [34].

Peterseim et al. made a comparison among current CSP technologies which are able to generate steam to hybridize with Rankine cycle power plants using gas, coal, biomass and waste material. Technologies are investigated in terms of feasibility (solar to electricity efficiency, operation range and maximum site gradient), risk (technical maturity, plant complexity and integration simplicity), environmental impact (land use and cleaning water consumption) and LCOE (levelized cost of electricity). Installed capacity is assumed as 10 MW_e and CSP contribution is taken as 20 MW_{th}. For a host plant using biomass and generating steam at 480 C, solar tower with direct steam generation scores best. In terms of technical maturity, parabolic trough technology using synthetic oil noticeably better than others [35].

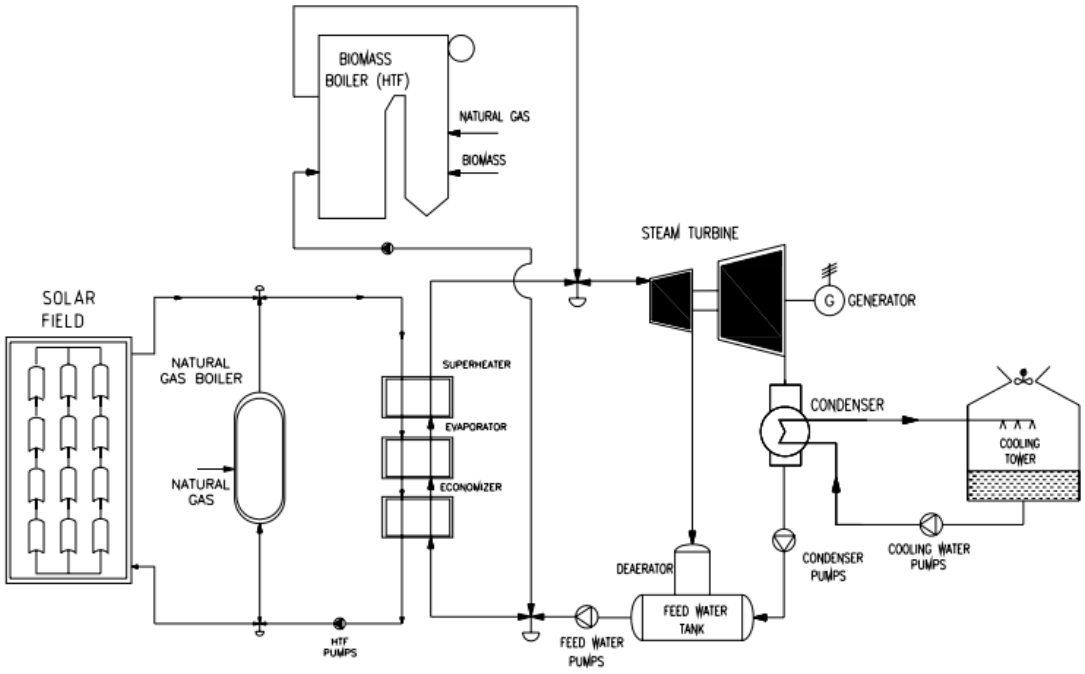

Figure 14 Solar-Biomass Hybrid Configuration with Parallel Connection

For another study, Peterseim et al. investigated 17 different mature CSP-biomass hybrid configurations with references over 5 MW_e in terms of technical, environmental and economic aspects. CSP technologies include PTC, LFR and ST whereas options for biomass conversion technologies contain grate furnaces, fluidized bed combustion systems and gasifiers. The best commercial option is hybridizing solar tower with fluidized bed. However, combination of solar tower with gasification gives the best result in technical and environmental evaluations. The research shows that the investment cost can be reduced up to 69% by hybridizing standalone CSP projects with biomass assuming that the annual electricity generations are the same for both systems [36].

Peterseim et al. considered hybridization options for CSP with other energy sources like coal, natural gas, biomass, etc. in several levels including feed water heating and steam reheating. Hybrid configurations are classified as light, medium and strong synergy systems which refer to the degree of interconnection of the plant components. Amount of cost reduction depends on the degree of interconnection. Moreover, strong synergy systems can better match their energy output with electricity pricing. Hence, energy sources sharing Rankine cycle components (steam turbine, condenser, etc.)

with CSP such as biomass and natural gas have more advantage compare to wind energy. The study focuses on Australia and results show that cost reduction up to 50% can be achieved by hybrid plants [37].

30 MW_e CSP-biomass hybrid plant with 3h thermal storage in Griffith, New South Wales investigated by Peterseim et al. Solar tower technology with molten salt is selected for CSP part with an installed power of 15 MW_e. Steam at 525°C and 120 bar is generated in both biomass boiler and solar tower. Investment cost is 43% lower compare to a standalone CSP plant with 15h storage capacity [38].

Bai et al. evaluated a solar biomass hybrid power generation system based on Rankine Cycle with an installed capacity of 50 MW. The system consists of parabolic trough collectors (pre-heater) with tracking, a biomass steam boiler and a power generation subsystem. In PTCs section, synthetic oil serving as a HTF is heated to 391°C and then used to produce steam at 371°C via heat exchangers. The steam is further heated to 540°C in the biomass boiler that burns cotton stalk having a lower heating value of 1764.8 kJ/kg [39].

According the results including thermal efficiency of the cycle and exergy analysis of the system, performance of the hybrid system is 3.89% greater than that of solar only system and amount of exergy loss due to biomass combustion in the hybrid system is 19.36% which is smaller than that of biomass only system, 49.39%. Preliminary economic performances of the system were also investigated in the study. Levelized Cost of Energy (LCOE) for the hybrid system was calculated as 0.077 $/kWh whereas it is 0.192 $/kWh for a solar only system [39].

Hussain et al. assessed the suitability of solar technologies, which includes Solar Tower, Parabolic Trough, Linear Fresnel and Solar Photovoltaic, for hybridization with biomass in Europe. Regarding the biomass conversion technologies, gasification and combustion are also evaluated in terms of their convenience for hybridization. Solar-biomass hybrid technology combinations were compared with standalone biomass and solar systems. The study shows that PTC is the most suitable technology for hybridization with biomass in Europe since the technology is more mature and economic compare to other alternatives. In terms of biomass, combustion is preferable due to its lower cost and proven technology. A hybrid parabolic trough-biomass

combustion power plant was simulated via TRNSYS 17. The simulation model shows that conventional fossil-fueled thermal power plants can be alternated by CSP-biomass hybrid power plants since the hybrid configuration increases capacity factors and decreases biomass consumption [40].

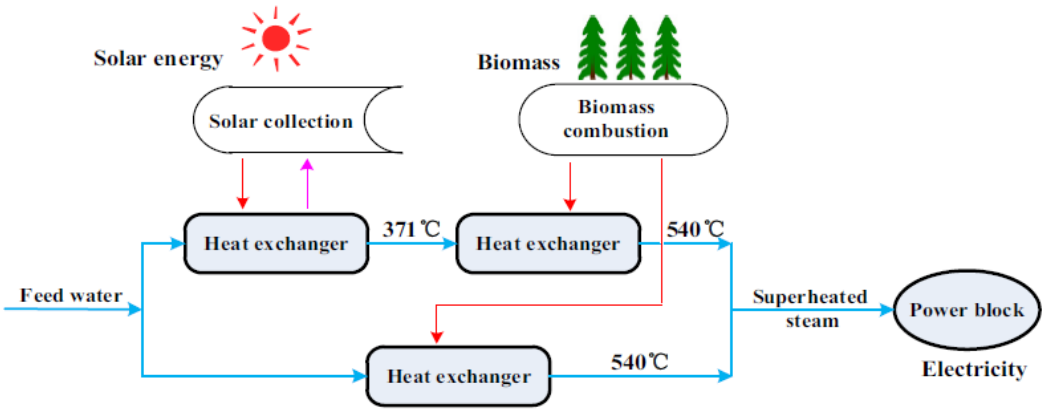

Figure 15 The Concept of the Solar-Biomass Hybrid System for Power Generation [39]

There are several studies on HTFs used in parabolic trough collectors. Ouagued et al. compared the outlet temperature profiles of Syltherm 800, Syltherm XLT, Therminol D12, Santotherm 59, Marlotherm SH and Marlotherm X in the Algerian climatic conditions [41].The said thermal oils were also evaluated according to their cost. The study shows that Syltherm 800 has the highest peak temperature (700-750 K) and it is followed by Marlotherm SH, Therminol D12 and Santotherm 59. The cost of Syltherm is between 30 and 60 US $/kg whereas aromatic synthetic oils like Marlotherm, Santotherm and Therminol are less expensive from about 1 to 10 US $/kg. HTFs should be highly stable and have good heat transfer properties at high temperature liquid phase. In addition to these, they should not be corrosive to construction materials.

Selvakumar et al. investigated several heat transfer fluids such as helium, therminol, calfo, duratherm, exceltherm, molten salt, dynalene and vegetable oil in terms of flow characteristics and heat transfer[42]. The best heat transfer fluid among them for short flow length applications is specified as Therminol. There are several grades of

Therminol, operating temperature limits are determinant for selection. Selvakumar et al. conduct a research on performance of collectors using Therminol D12 as HTF [43]. The study showed that Therminol D12 with 62°C of flash point is suitable for the systems designed for low solar irradiance. Operating temperature limits of other Therminol heat transfer fluids are given in Figure 16 [44]. Therminol 62, Therminol 66 and Therminol VP-1 are suggested for CSP applications. As can be seen from the figure, Therminol VP-1 has the maximum operating temperature, 400°C, among others and it is preferred as HTF in most of the studies [45]–[47].

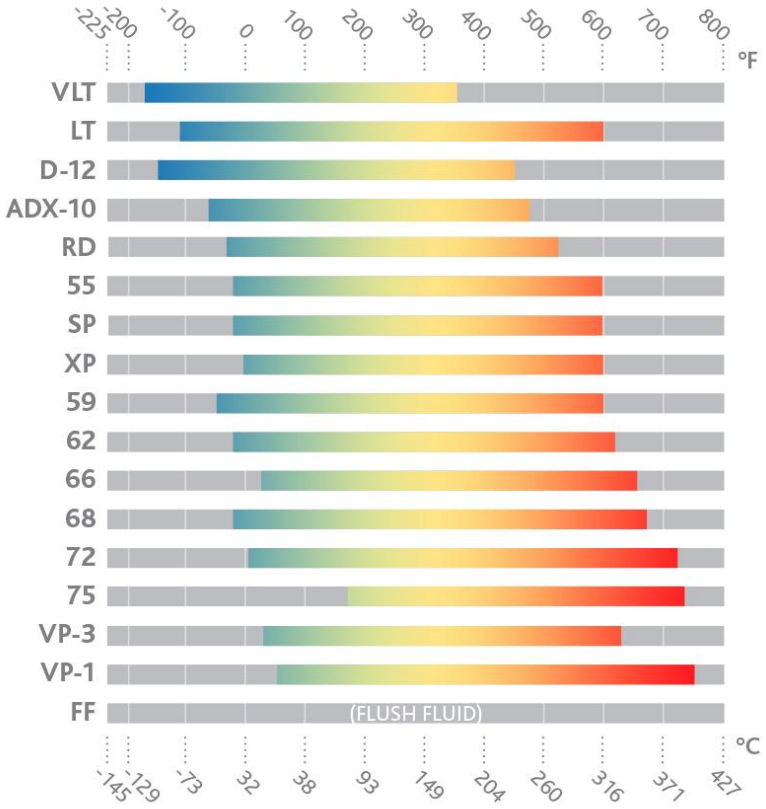

Figure 16 Operating Temperature Limits of Therminol®[44]

In this study, turbine inlet temperature and pressure, operating temperature range and pressure of the HTF, collector efficiency and heat loss ratio in the collectors are selected according to the current literature.

CHAPTER 3

SIMULATION MODEL

For the purpose of this study a hybrid solar-biomass power plant model is developed using ASPEN PLUS software. ASPEN is a process simulation software package. Given a process design and an appropriate selection of thermodynamic models, ASPEN uses mathematical models to predict the performance of the process. The program takes a design that the user supplies and simulates the performance of the process specified in that design. ASPEN PLUS is one of the ASPEN packages which is used for the steady-state process simulations. The system is based on "blocks" corresponding to unit operations. Materials, work and heat streams are used to interconnect the blocks and construct the flow sheet. Flow rates, composition and operating conditions must be specified for the inlet streams. In order to complete the flow sheet, operating conditions such as temperature, pressure, vapor fraction, etc. must be stated for the blocks and heat/work inputs into the process must be also specified.

The hybrid power plant is continuously operated on a simple steam Rankine cycle. During day time, the steam is generated from two sources. However, during night time, only biomass energy can be utilized to generate steam.

A simple Rankine cycle consists of a steam turbine, pump and heat exchangers (boiler and condenser) [48]. In the proposed Rankine cycle, there are two separate systems (solar field and biomass boiler) which transfer heat to the water in order to obtain steam. They are considered as the boiler of the power plant.

Input and output parameters shown in Table 2 are used in this study. General schematic of the Hybrid Power Plant is shown in Figure 25 and Figure 26.

Table 2 Input and Output Parameters

Input Parameters	**Output Parameters**
DNI values	Mass flow rate of water in CSP
Collector area & efficiency	Mass flow rate of water in boiler
Heat loss to the surrounding	Mass flow rate of HTF
Water inlet temperature and pressure	Mass flow rate of biomass
HTF inlet & exit temperature and pressure	CO_2 Emission
Turbine inlet temperature	
Pump exit pressure	
Turbine work	
Biomass Ultimate and Proximate analysis	
Biomass Moisture Content & Heating Value	

For the selected installed capacities, two different simulations are performed. As explained in Section 2.2.2., operating temperatures of heat transfer fluids are limited and the upper limit is around 400°C. Therefore, solar collectors are not able to heat the steam over 400°C. Two different solution are suggested to overcome this problem and two simulation model are performed to analyze each solution.

- Solution-1 : Add Auxiliary Boiler (CASE – I)
- Solution-2 : Increase Biomass Boiler Load (CASE – II)

Simulation model is composed of 6 sub-systems for CASE – I: Solar field, Biomass boiler, Steam turbine, Condenser, Pump and Auxiliary boiler. For CASE – II, there are 5 components and no auxiliary boiler.

CASE-1: An auxiliary boiler using methane as fuel is installed at the exit of the solar field to superheat the steam leaving the collectors. General schematic of CASE-1 is indicated in Figure 18.

CASE-2: In Case-2, solar field steam is mixed with superheated steam coming from biomass boiler. By changing the feed rate of biomass, thermal equilibrium temperature of the mixture is set a value which is above the turbine inlet temperature. Figure 17 shows the general layout of CASE-2.

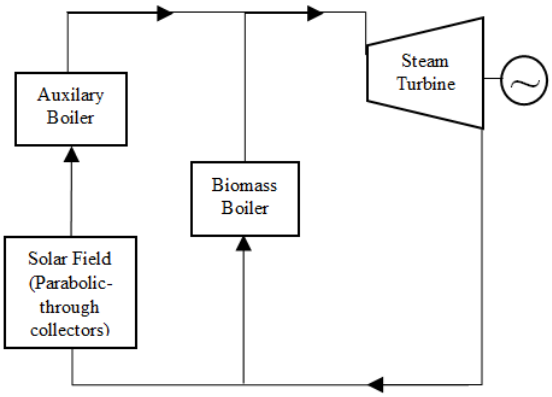

Figure 18 General Schematic of CASE-1

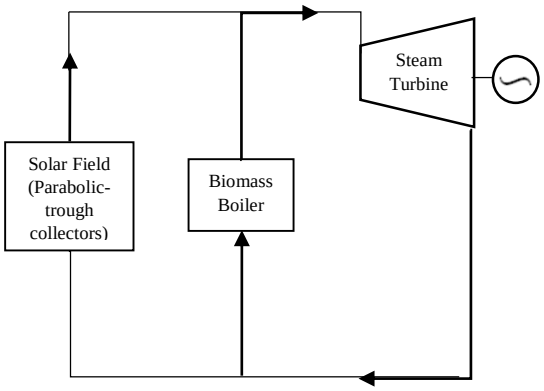

Figure 17 General Schematic of CASE-2

A brief description of the process components and operating conditions are given in the following sections. Details about usage of each block diagram in Aspen Plus is given in Appendix- A.

3.1 Solar Field

Kırklareli region is selected (explained in Section 1.3) for the power plant location. DNI values for Kırklareli region through one year period is given in Appendix-B [49]. Considering the DNI values, total collector area is set as 5,000 m^2 to satisfy the required heat input.

CSP technologies and their operating principals are covered in Section 1.1. PTCs system operating with a heat transfer fluid is utilized in solar part. Based on the conducted studies evaluating the performance characteristics of parabolic trough

collectors [8], [50]–[52], collector field efficiency is assumed as 70% and thermal heat loss is taken as 10%.

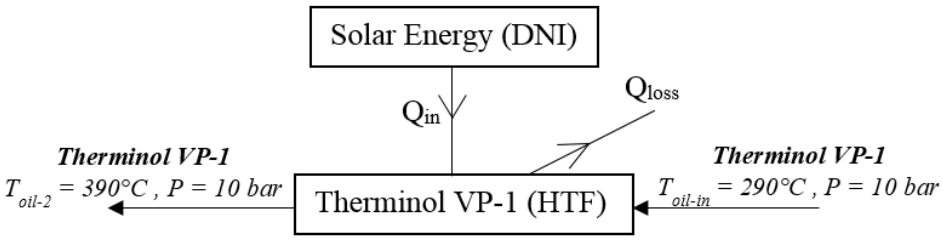

Figure 19 Schematic of heat transfer process in PTC

Therminol VP-1 is selected as the heat transfer fluid in this study since it has the upper limit in terms of operating temperature (400°C) among other available HTFs. Figure 19 shows the schematic of heat transfer process in PTC. Therminol VP-1 exit temperature is set as 390°C at 10 bar to be on the safe side.

Heat input rate to the heat transfer fluid can be calculated by using the following equation:

$$Q_{in} = DNI * Collector\ Area * \eta_{collector} * (1 - \eta_{heatloss}) \qquad (1)$$

As a simple calculation for 400 W/m^2 DNI value, Q_{in} is found as 1.26 MW;

$$Q_{in} = 400 * 5000 * 0.7 * (1 - 0.1) = 1{,}260{,}000\ W = 1.26\ MW$$

Figure 20 shows the schematic of heat transfer process between HTF and water. Water inlet temperature is taken as the ambient temperature which is 25°C. Evaporation takes place in the heat exchanger at constant pressure which is equal to turbine inlet pressure (40 bar). Depending on the HTF exit temperature, steam exit temperature is set as 389°C.

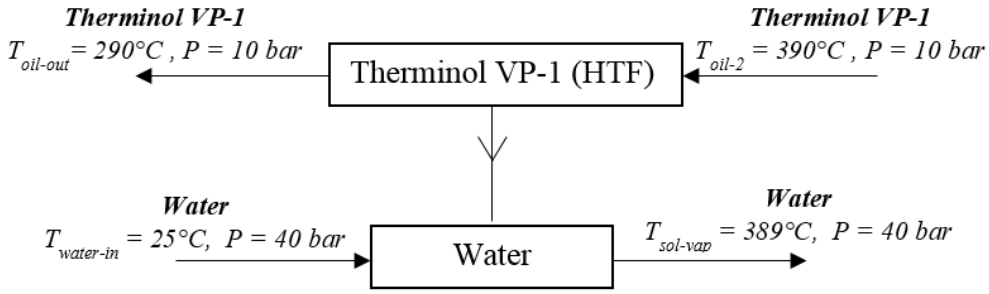

Figure 20 Schematic of heat transfer process between HTF and water

As can be seen from Appendix-B, DNI values are changed seasonally and daily. In other words, the thermal energy transferred to the HTF is not constant. Moreover, fluctuations in ambient temperature and wind speed cause disturbances on HTF in practice. Control strategies are employed to keep the steam temperature near its set point and to keep collector outlet temperature of HTF below 390°C to prevent oil from getting close to the maximum bulk use temperature. The common method in several control strategies is setting the HTF mass flow rate as manipulated variable which is used to control the HTF temperature after passing through the PTCs[47].

3.2 Biomass Boiler

As mentioned in Section 1, direct combustion method is used to obtain steam for Rankine cycle. Forest based biomass with low moisture content is suitable for direct combustion. Considering its availability, cost and chemical properties, woodchips are selected as biomass source in this study.

Net energy content of the biomass mainly depends on the moisture content. Moisture content of the selected biomass is around 20% [54], [55]. Chemical composition of the biomass affects the combustion performance. Important factors affecting the combustion performance are ash, carbon, hydrogen, nitrogen, sulphur, oxygen and chloride content of the biomass. The higher carbon and hydrogen content lead to a higher heating value whereas high oxygen content leads to a high reactivity at normal combustion temperatures and this cause more rapid combustion [56]. Selected biomass contains very low amount of nitrogen and no sulphur. Therefore, NO_x emission produced after combustion shall be very low and there will be no SO_x emission.

Ultimate Analysis and Proximate Analysis together with the heating value of the selected biomass should be defined to ASPEN PLUS. Input values entered to Ultanal attributes (on dry basis) and heating value of the biomass are given in Table 3 whereas input values of Proxanal attributes are given in

Table 4. Sulfanal attributes are zero since the sulphur content of said biomass is zero. It should be noticed that the Ultanal value for ash equals to the proxanal value for ash. Ultanal values and Proxanal values for FC, VM and ash sum to 100.

Table 3 Ultanal Attributes Input Values

Ultimate Analysis	**Percentage %**
Ash	0.2
Carbon	48.2
Hydrogen	6.0
Nitrogen	0.1
Sulphur	0.0
Oxygen	45.5
Chloride	0.0
Heating Value (MJ/kg)	19

Table 4 Proxanal Attributes Input Values

Proximate Analysis	**Percentage %**
Ash	0.2
FC (fixed carbon)	14.8
VM (volatile matter)	85.0
Moisture	20

Combustion air is assumed to be composed of oxygen (O_2) and nitrogen (N_2) with mole fractions of 0.79 and 0.21 respectively. Inlet temperature of the air is taken as the ambient temperature (25°C) whereas the pressure is taken as the atmospheric pressure (1 bar).

There are 3 stages in the biomass boiler: Economizer, Evaporator and Superheater. Schematic of the processes in the biomass boiler is shown in Figure 21.

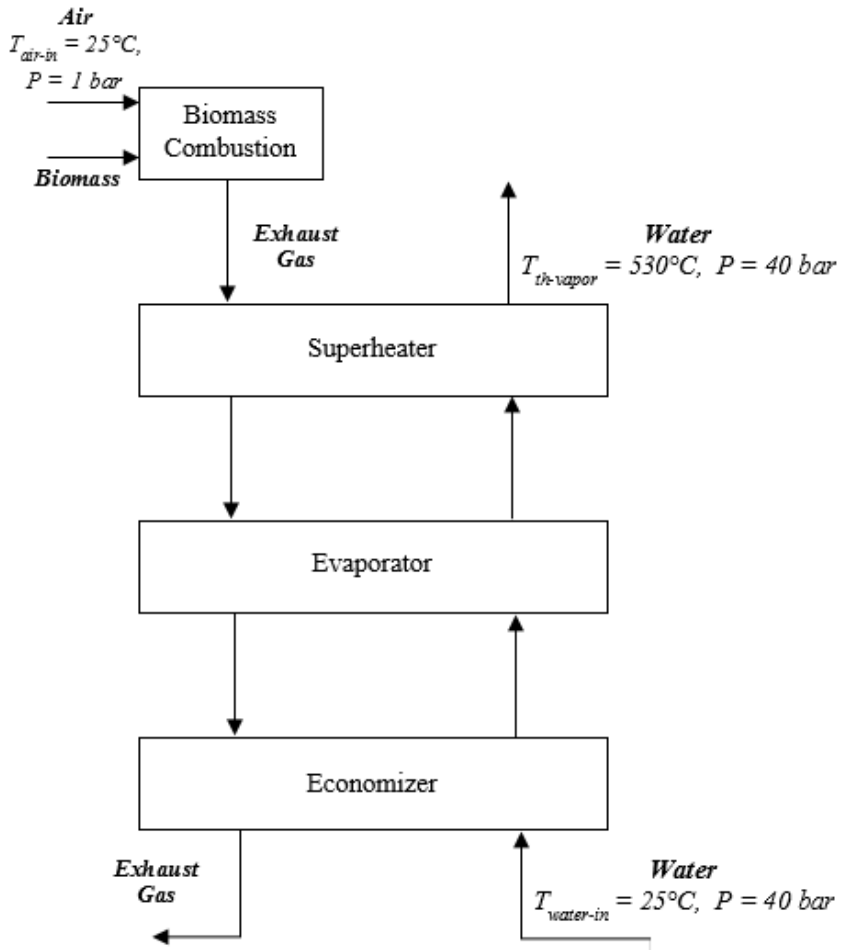

Figure 21 Schematic of Biomass Boiler Stages

Inlet water heated up at constant pressure to its boiling point in the economizer. Phase change occurs in the evaporator stage. Specifications of the superheater section is different for each cases. In CASE – I (with auxiliary boiler), superheater heats the vapor to 530°C (turbine inlet temperature). In CASE – II, superheater exit temperature is controlled and increased up to a temperature at which the vapor mixture, formed by the vapor coming from the solar field and the biomass boiler, reaches the turbine inlet temperature. In order to have a constant work output from the steam turbine and to maintain the vapor temperature at 530°C, mass flow rate of biomass is varied according to the DNI values.

3.3 Steam Turbine

According to Desai et al. the turbine inlet pressure is taken as 40 bar for the optimal turbine operation for 1 MW_e solar power plant based on a Rankine cycle [30]. Turbine inlet temperature and condensing pressure are determined by using commercial 1 MW steam turbine data [57]. Turbine inlet temperature is 530°C and inlet pressure is 40 bar. Isentropic and mechanical efficiencies of the turbine is taken as 85% and 98% respectively. Turbine exit pressure is 0.1 bar which leads a pressure ratio of 400.

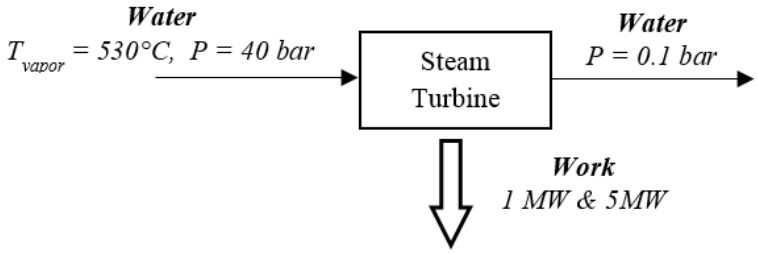

Figure 22 Schematic of the Steam Turbine

3.4 Condenser

Schematic of the condenser is shown in Figure 23. Phase change occurs at constant pressure and the saturated liquid at 0.1 bar leaves the condenser.

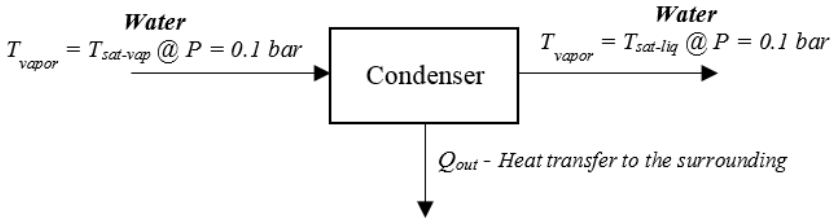

Figure 23 Schematic of the Condenser

3.5 Pump

Pump increases the pressure of saturated liquid from 0.1 bar to the boiler pressure level (40 bar). Isentropic efficiency of the pump is taken as 85%. Schematic of the pump is shown in Figure 24.

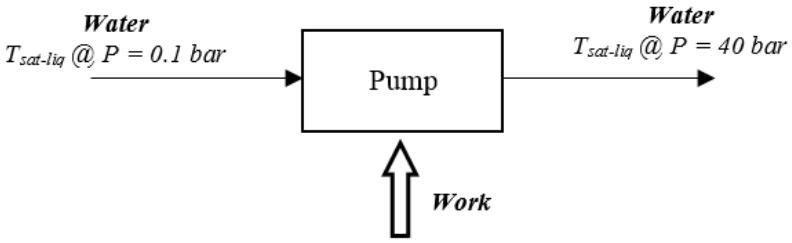

Figure 24 Schematic of the Pump

3.6 Auxiliary Boiler (for CASE-1)

The oil temperature (max. 390°C) is not high enough to produce steam at 530°C (turbine inlet temperature). Therefore, steam must be superheated by using either an auxiliary boiler or the steam coming from the biomass boiler (CASE-2). Both options are examined in this study.

In CASE–I, a methane fired auxiliary boiler is used to superheat the steam leaving the solar field. Modelling of the auxiliary boiler is similar to that of biomass boiler. Fuel load of the auxiliary boiler is controlled to obtain a constant steam temperature at the exit of the boiler dependent from the DNI values. Mass flow rate of methane is changed according to the mass flow rate of the water.

In CASE–II, the steam leaves the super-heater part of the biomass boiler above the turbine inlet temperature and then mixed with the steam coming from the solar field. As a result of mixing, an equilibrium temperature of 540°C is reached.

Some of the selected input parameters for the simulation are given in Table 5. Figure 25 is taken from ASPEN PLUS user face and indicates the general layout of the simulation for CASE-I. There are 6 subsystems which are marked with the red lines in the figure. Figure 26 shows the general layout for CASE-II. The only difference between general layouts of CASE-I and CASE-II is the auxiliary boiler (subsystem #6).

Table 5 Input Parameters for the Hybrid System Simulation

Input Parameter	**Value/Type**
Installed Capacity	1 MW
Place	Kırklareli (Turkey)
Collector field	Parabolic Trough Collector
Biomass Field	Direct Combustion - Inclined Grate
Biomass Source	Woodchips
Collector aperture area	5,000 m^2
Collector field efficiency	70%
Heat transfer fluid	Therminol VP-1
Collector outlet temperature	390 °C
Ambient temperature	25 °C
Turbine inlet pressure	40 bar
Turbine inlet temperature	530 °C
Turbine isentropic efficiency	85%
Pump hydraulic efficiency	70%
Condensing pressure	0.1 bar

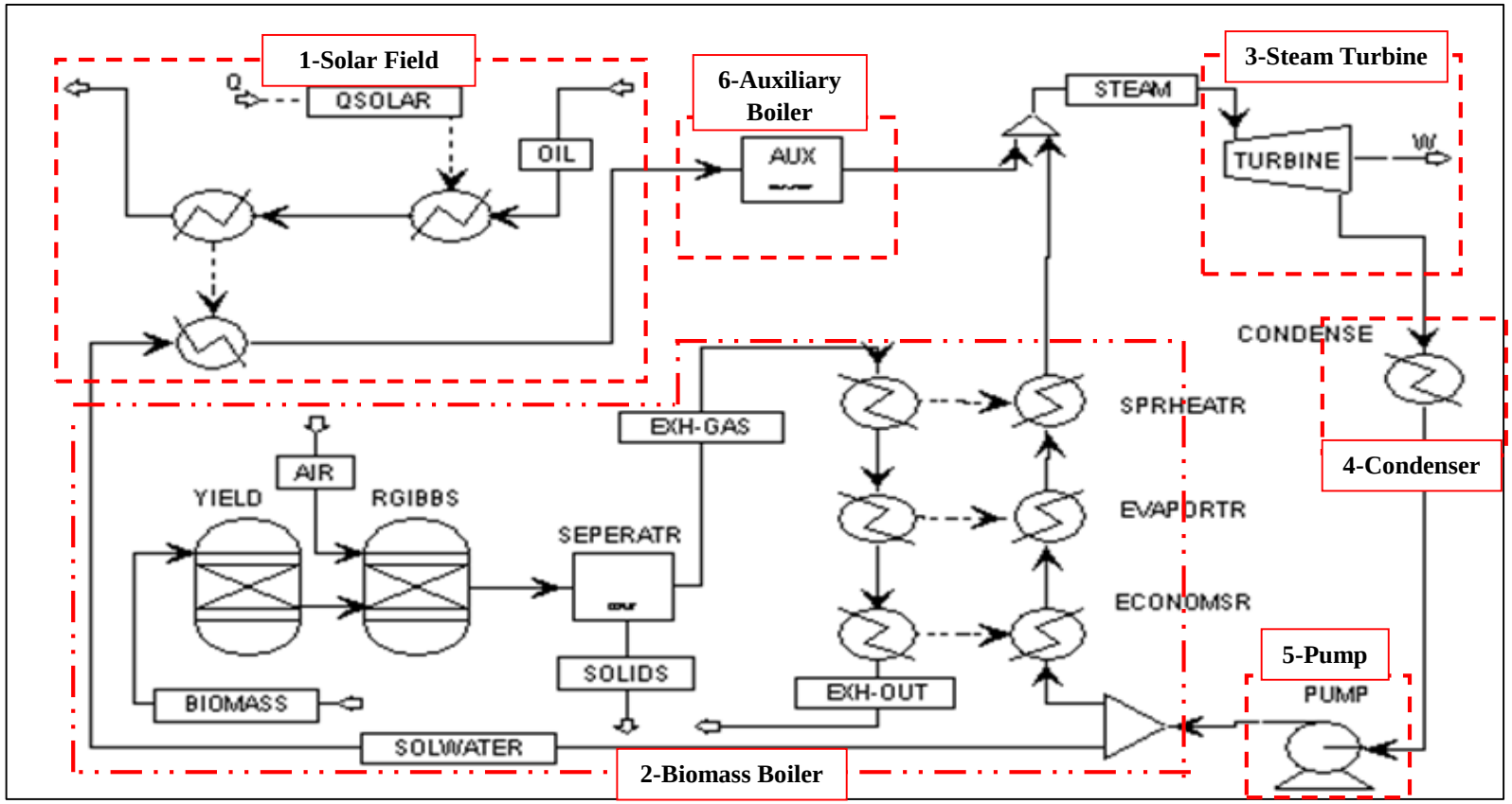

Figure 25 ASPEN PLUS's Block Diagram Layout for CASE – I

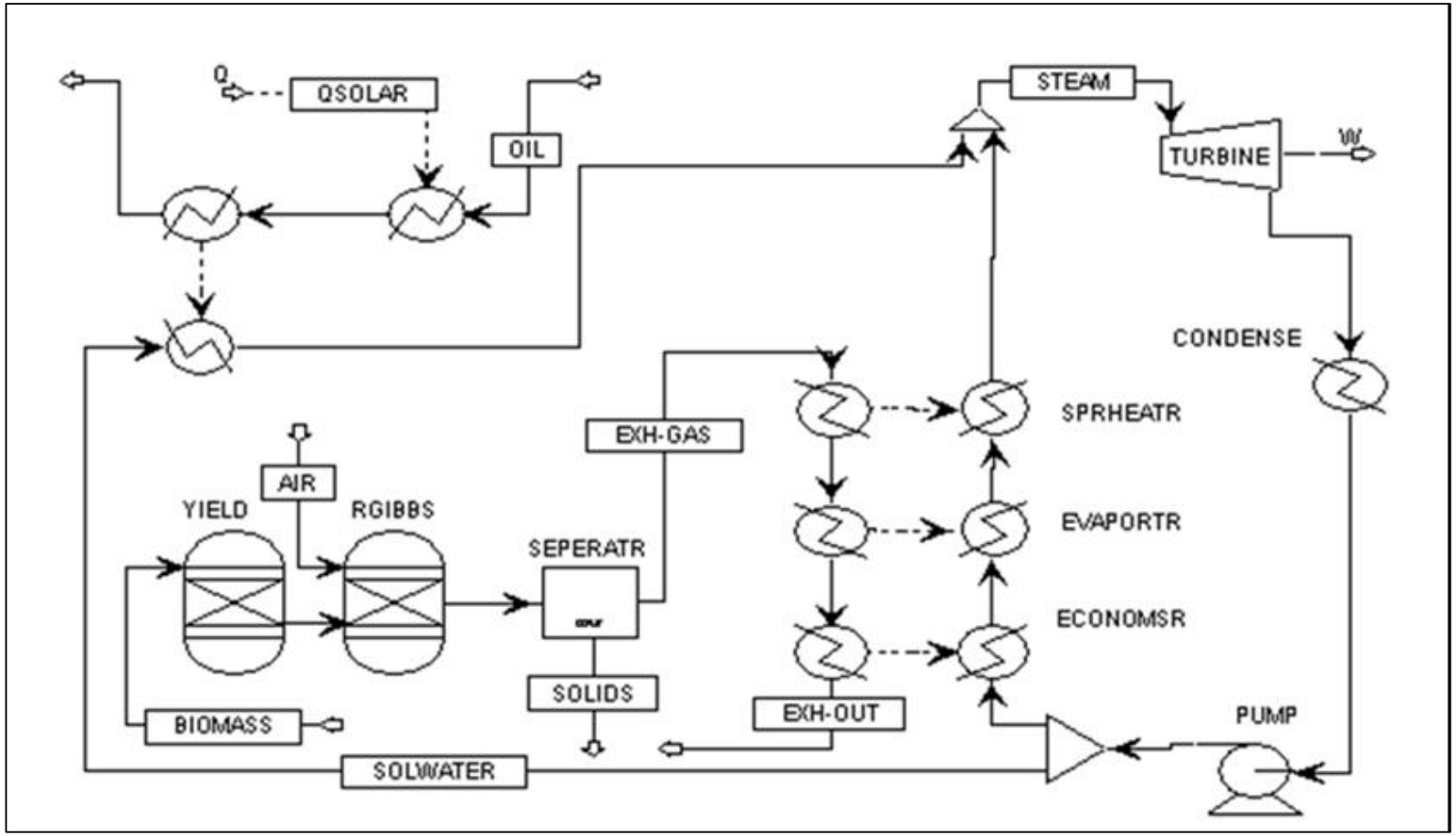

Figure 26 ASPEN PLUS's Block Diagram Layout for CASE – I

CHAPTER 4

RESULTS

Simulation models formed for CASE-1 and CASE-II are run for both 1 MW and 5 MW installed capacities and all DNI values throughout the year. Mass flow rates of HTF, water in solar collectors, water in biomass boiler, biomass and methane are obtained together with the total CO_2 emission for each case and size during one year period.

As the DNI values increase, the amount of thermal energy input to the system from solar field also increases. Therefore, the amount of HTF and the amount of water to be heated by this thermal energy getting higher. In other words, the mass flow rate of the heat transfer fluid (M_{oil}) and the mass flow rate of the water in the solar field ($M_{s\text{-}water}$) increase with DNI values. The more the amount of water means the more amount of methane required to superheat that water. So, the mass flow rate of the methane is proportional to the mass flow rate of water in the solar field. On the other hand, mass flow rate of biomass is inversely proportional to the DNI values since less thermal energy requires from biomass boiler as the solar energy input increases.

For 1 MW installed capacity; mass flow rates for selected DNI values for CASE – I and CASE – II are given in Table 6 and In CASE–II, required energy to superheat the water in the solar field is met by increasing the thermal energy input supplied by the biomass boiler. Hence, mass flow rate of biomass in CASE–II is higher than that of CASE-I for the same DNI value.

Table 7 respectively. Unit of the mass flow rates is kilogram per second whereas the DNI values are given in watt per square meter.

Table 6 Mass Flow Rates for selected DNI values / CASE-I (1 MW)

DNI (W/m^2)	M_{oil} (kg/s)	$M_{s\text{-}water}$ (kg/s)	$M_{b\text{-}water}$ (kg/s)	$M_{biomass}$ (kg/s)	$M_{methane}$ (kg/s)
300	3.92	0.32	0.64	0.24	0.006208
400	5.23	0.42	0.54	0.20	0.008143
500	6.60	0.53	0.44	0.16	0.010286
600	7.85	0.64	0.33	0.12	0.012421

In CASE–II, required energy to superheat the water in the solar field is met by increasing the thermal energy input supplied by the biomass boiler. Hence, mass flow rate of biomass in CASE–II is higher than that of CASE-I for the same DNI value.

Table 7 Mass Flow Rates for selected DNI values / CASE-II (1 MW)

DNI (W/m^2)	M_{oil} (kg/s)	$M_{s\text{-}water}$ (kg/s)	$M_{b\text{-}water}$ (kg/s)	$M_{biomass}$ (kg/s)
300	3.92	0.32	0.64	0.25
400	5.23	0.42	0.54	0.21
500	6.60	0.53	0.44	0.18
600	7.85	0.64	0.33	0.14

For 1 MW installed capacity; CO_2 emission of CASE – I and CASE – II for selected DNI values are given in Table 8. Unit of the CO_2 is kilogram per second. It is seen that for the same amount of fuel, CO_2 emission from methane is higher than the CO_2 emission of biomass. For CASE-I, 98% of the total emission is caused by the biomass boiler. Comparing the total emission for CASE-I and CASE-II, CASE-I's emission is slightly higher than that of CASE-II.

Table 8 CO_2 Emission for CASE – I and CASE – II (1 MW)

DNI (W/m^2)	CASE - I			CASE II
	CO_2 from biomass (kg/s)	CO_2 from methane (kg/s)	Total CO_2 (kg/s)	Total CO_2 (kg/s)
300	0.3384	0.0170	0.3554	0.3525
400	0.2820	0.0223	0.3043	0.2961
500	0.2256	0.0282	0.2538	0.2538
600	0.1692	0.0341	0.2033	0.1974

For 5 MW installed capacity; mass flow rates for selected DNI values for CASE – I and CASE – II are given in Table 9 and
Table 10 respectively.

Table 9 Mass Flow Rates for selected DNI values / CASE-I (5 MW)

DNI (W/m^2)	M_{oil} (kg/s)	$M_{s\text{-}water}$ (kg/s)	$M_{b\text{-}water}$ (kg/s)	$M_{biomass}$ (kg/s)	$M_{methane}$ (kg/s)
300	7.85	0.64	4.20	1.52	0.012421
400	10.46	0.85	3.99	1.44	0.016498
500	13.08	1.06	3.78	1.37	0.020574
600	15.69	1.27	3.57	1.29	0.024654

Table 10 Mass Flow Rates for selected DNI values / CASE-II (5 MW)

DNI (W/m^2)	M_{oil} (kg/s)	$M_{s\text{-}water}$ (kg/s)	$M_{b\text{-}water}$ (kg/s)	$M_{biomass}$ (kg/s)
300	7.85	0.64	4.20	1.54
400	10.46	0.85	3.99	1.47
500	13.08	1.06	3.78	1.40
600	15.69	1.27	3.57	1.33

For 5 MW installed capacity; CO_2 emission of CASE – I and CASE – II for selected DNI values are given in Table 11.

Table 11 CO_2 Emission for CASE – I and CASE – II (5 MW)

DNI (W/m^2)	CASE - I			CASE II
	CO_2 from biomass (kg/s)	CO_2 from methane (kg/s)	Total CO_2 (kg/s)	Total CO_2 (kg/s)
300	2.1432	0.034075	2.1773	2.1714
400	2.0304	0.045259	2.0757	2.0727
500	1.9317	0.056441	1.9881	1.9740
600	1.8189	0.067633	1.8865	1.8753

Annual biomass consumption, annual CO_2 emission and annual methane consumption are calculated by using mass flow rates. For a given day, DNI values of the corresponding hours are known so that biomass and methane consumption and CO_2 emission for that hour can be calculated by simple multiplying the mass flow rate with 3600 (second/hour). For an hour at which the DNI value is 400 W/m^2, biomass and methane consumption and CO_2 emission for CASE-I is;

$$Biomass = M_{biomass} * 3600 = 0.20\left(\frac{kg}{s}\right) * 3600\ \left(\frac{s}{h}\right) = 720\ kg/h$$

$$CO_2 = M_{CO2} * 3600 = 0.3043\ \left(\frac{kg}{s}\right) * 3600 = 1095.48\ kg/h$$

$$Methane = M_{methane} * 3600 = 0.008143\left(\frac{kg}{s}\right) * 3600\ \left(\frac{s}{h}\right) = 29.32\ kg/h$$

Density of the methane is 0.6443 kg/m^3 so, the methane consumption in terms of m^3/kg can be calculated as;

$$Methane\ \left(\frac{m^3}{h}\right) = \frac{Methane\left(\frac{kg}{h}\right)}{0.6443\left(\frac{kg}{m^3}\right)} = \frac{29.32}{0.6443} = 45.51\ m^3/h$$

For both CASE-I and CASE-II, the above calculation is made for each hour of the year and the annual biomass consumption, CO_2 emission and methane consumptions are shown in the following section.

4.1 Annual Biomass Consumption

Mass flow rate of biomass fuel is obtained for different DNI values. As the DNI increases, contribution from solar field to the generated steam amount rises. As a result, biomass requirement of the system decreases and biomass consumption rate becomes lower.

Monthly biomass fuel consumption amount of the hybrid power plant with an installed capacity of 1 MW are obtained through one year period and separately displayed for CASE – I and CASE – II in Figure 27. Vertical axis indicates the consumption amount in tons/month whereas the horizontal axis shows the months. Results for 5 MW hybrid power plant is given in Figure 28.

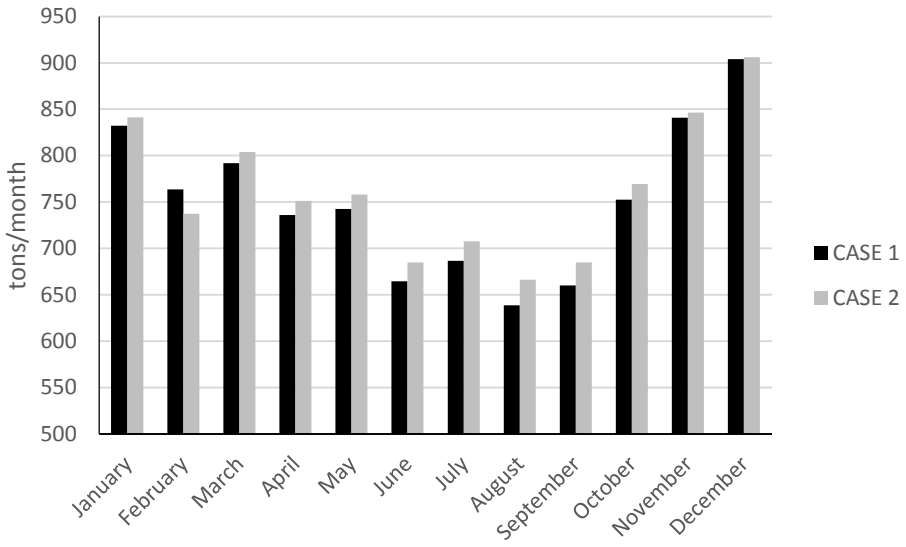

Figure 27 Monthly biomass consumption amount for CASE–I and CASE–II (1 MW)

Total biomass consumption for CASE-I and CASE-II are 9,012 tons/year and 9,157 tons/year respectively. It is seen that the biomass consumption is lower in summer months, where the solar energy is high, and higher in winter months compare to the annual average. As it is expected due to the sunshine hours and DNI values of Kırklareli, August has the lowest biomass consumption amount and December has the highest. Fuel consumption rate of biomass only power plant with 1 MW installed

capacity is also calculated. In order to give the same output power as hybrid power plant, 11069 tons biomass is burnt annually.

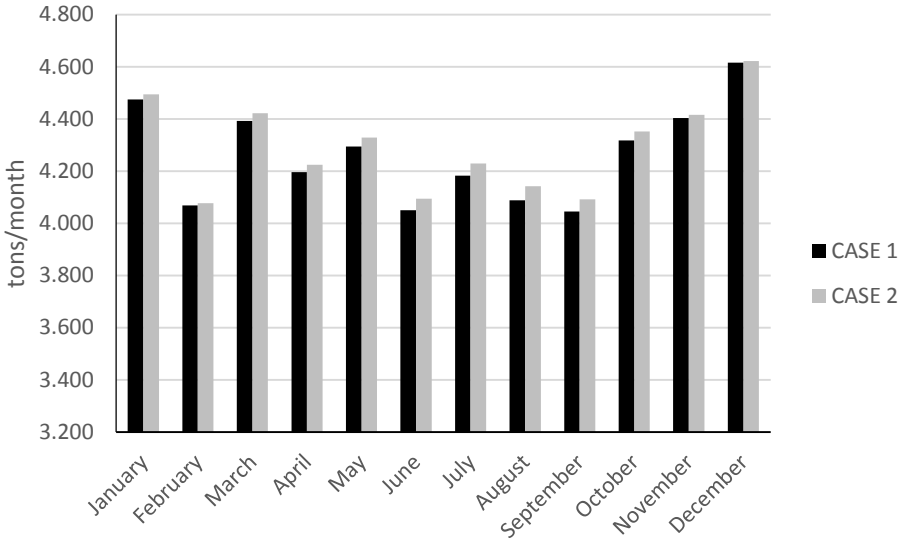

Figure 28 Monthly biomass consumption amount for CASE–I and CASE–II (5 MW)

Total biomass consumption for CASE-I and CASE-II are 51,127 tons/year and 51,490 tons/year respectively. Results for 5 MW installed capacity has the same trend with the results found for 1 MW installed capacity. Biomass consumption for 5 MW is not 5 times the biomass consumption of 1 MW since the solar collector area for 5 MW is not scaled 5 times compare to the area selected for 1 MW. Fuel consumption rate of biomass only power plant with 5 MW installed capacity is 55,188 tons/year.

4.2 Annual CO_2 Emission

CO_2 emissions of the biomass boiler and the auxiliary boiler are also investigated. Monthly CO_2 amount released by the hybrid power plant with an installed capacity of 1 MW are obtained through one year period and separately displayed for CASE – I and CASE – II in Figure 29. Results for 5 MW hybrid power plant is given in Figure 30.

CO_2 emission of CASE-I is slightly higher than that of CASE-II. Total CO_2 emission for CASE-I and CASE-II are 13,009 tons/year and 12,911 tons/year respectively As the contribution of solar field increases, in summer months, CO_2 emission of the power plant decreases: As in the results for biomass consumption, August has the lowest

emission value whereas December has the highest. CO_2 of biomass only power plant with 1 MW installed capacity is also calculated. In order to give the same output power as hybrid power plant, 15608 tons of CO_2 is released.

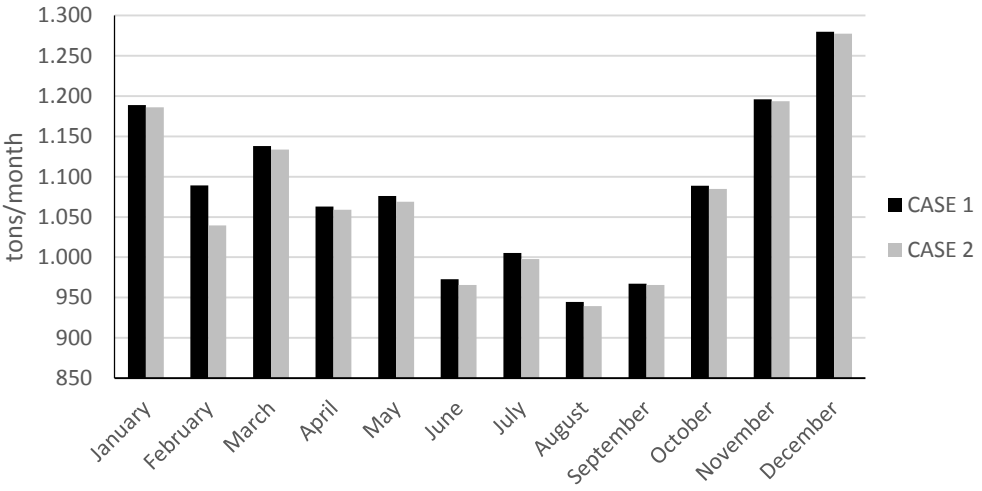

Figure 29 Monthly CO_2 emission for CASE–I and CASE–II (1 MW)

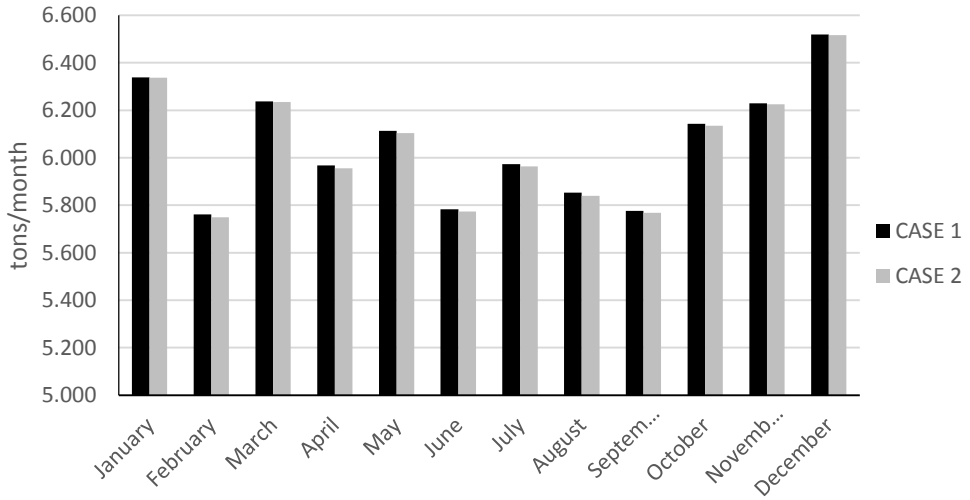

Figure 30 Monthly CO_2 emission for CASE–I and CASE–II (5 MW)

Total CO_2 emission for CASE-I and CASE-II are 72,691 tons/year and 72,601 tons/year respectively. Results for 5 MW installed capacity has the same trend with the results found for 1 MW installed capacity. CO_2 of biomass only power plant with

5 MW installed capacity is also calculated. In order to give the same output power as hybrid power plant, 77,815 tons of CO_2 is released.

4.3 Annual Methane Consumption

For CASE-I, annual methane consumption of the auxiliary boiler is calculated for both 1 MW and 5 MW installed capacities. Monthly methane consumption the hybrid power plant with an installed capacity of 1 MW is given in Figure 31. Results for 5 MW hybrid power plant is given in Figure 32.

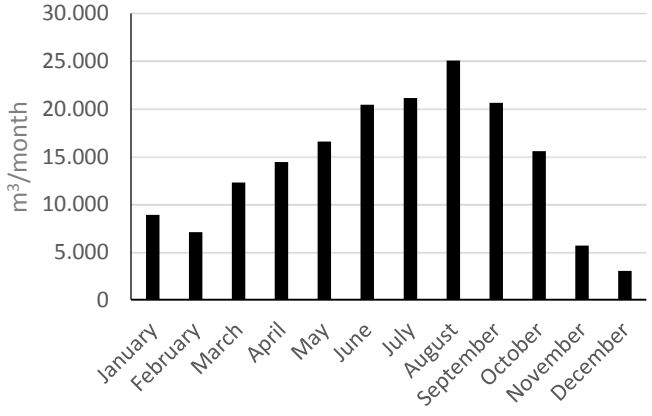

Figure 31 Monthly methane consumption amount for CASE–I (1 MW)

Methane consumption increases in summer months where the auxiliary boiler is used more often than winter months. Total methane consumption is 170,857 m3/year which has the highest value in August and the lowest value in December.

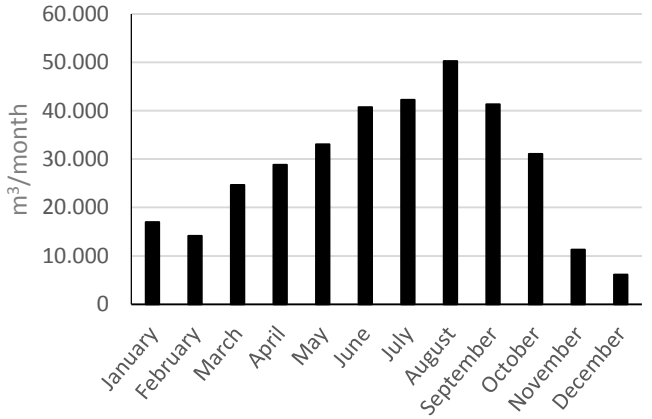

Figure 32 Monthly methane consumption amount for CASE–I (5 MW)

Total methane consumptions for 5 MW installed capacity is 340,749 m^3/year and the monthly distribution has a similar trend with that of 1 MW installed capacity.

4.4 Thermal Efficiency of the Rankine Cycle

Thermal efficiency of the Rankine cycle for CASE-II is calculated. Average DNI value for the selected place is 400 W/m^2 and the total solar area is 5000 m^2. Considering 70% overall collector efficiency and 10% heat loss to the surrounding, heat input to the solar field can be calculated by using Equation (1) and found as 1260 kW.

$$Q_{solar} = 400 * 5000 * \ 0.7 * (1 - 0.1) = 1{,}260{,}000\ W = 1.26\ MW$$

Average biomass consumption rate of the cycle can be calculated by dividing the annual biomass consumption to the annual working hours. Annual biomass consumption is 9,157 ton for 1 MW hybrid power plant without auxiliary boiler and annual working hours is 8760h. So, the average biomass consumption rate can be found as 0.29 kg/s.

$$M_{biomass,avg} = \frac{9157}{8760} = 1.045\frac{ton}{hour} = 0.29\ kg/s$$

Lower heating value of the biomass is assumed as 19,000 kJ/kg, therefore, heat input to the biomass boiler can be calculated as 5510 kW.

$$Q_{biomass} = 19000 * 0.29 = 5510\ kW$$

Required pump work for the cycle operation is 28 kW and turbine output work is designed as 1000 kW. Utilizing these information, thermal efficiency can be calculated with the following equation;

$$\eta_{thermal} = \frac{w_{turbine} - w_{pump}}{q_{biomass} + q_{solar}} \quad (2)$$

$$\eta_{thermal} = \frac{1000 - 28}{5510 + 1260} = 0.1435$$

Thermal efficiency of the Rankine cycle is found as 14.35%.

CHAPTER 5

FINANCIAL ANALYSIS

The financial analysis for the hybrid system described in detail in Section 3 has been performed for both 1 MW and 5 MW installed capacities. In order to make a financial evaluation, different criteria have been calculated via the Financial Model using MS Excel. General assumptions and parameters used in the financial model are given in Table 12.

5.1 Investment Size and Used Technology

Installed capacity should be selected in order to perform a financial evaluation. Capital and Operational Expenditures, land size and annual generation amount are based on that selected installed capacity. In this study, Financial Model has been used for both 1 MW and 5 MW installed capacities.

As mentioned in Section 3, the hybrid system is based on concentrated solar power, parabolic trough collectors (PTCs) and direct biomass combustion technologies. In the financial analysis, the configuration with auxiliary boiler is not taken into consideration.

5.2 Total Annual Generation

During night time and in the day time to support the solar part, biomass part of the proposed hybrid system will be operating. Therefore, the hybrid power plant will have a capacity factor that equals the capacity factor of a standalone biomass fired power plant.

Capacity factors of selected technologies are given in Figure 33. As shown in the figure, capacity factor for biomass fired power plant is 84%. As a result, total annual generation for 1 MW installed capacity is 7’358 MWh and 36’792 MWh for 5 MW installed capacity.

Table 12 Financial Model Parameters

Parameter	**Value**	**Notes**
Currency	US Dollar ($)	Currency used in the relevant legislation
Investment Size	1 MW & 5 MW	Explained in Section 5.1
Financial Model Period	25 years	Economic life of the system
Inflation Rate	2.10%	U.S Consumer Price Index (CPI)[58]
Tax	20%	Corporate Tax Ratio in Turkey[59]
Amortization Period	10 years	Depreciation Unit List [60]
Amortization Rate	10%	
Land Requirement	27.4 m^2/kW	Explained in Section 5.4
CAPEX	5,961 $/kW	Explained in Section 5.4
OPEX (fixed)	26 $/kW	Explained in Section 5.5
OPEX (variable)	5.4 $/MWh	Explained in Section 5.5
Capacity Factor	84%	Explained in Section 5.2
Sales Price	113 $/MWh	Explained in Section 5.3

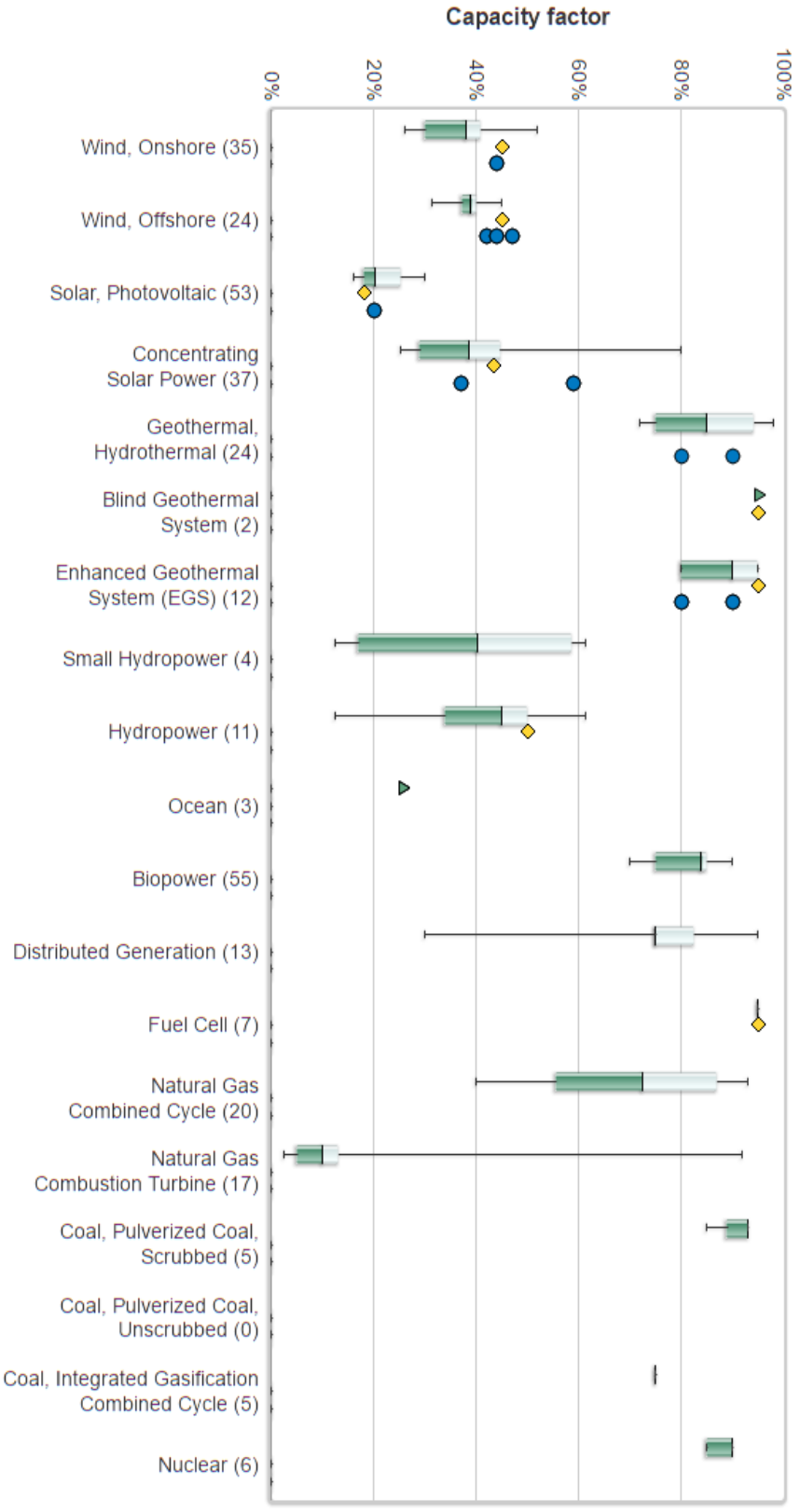

Figure 33 Capacity Factor of Selected Electricity Generation Technologies [61]

5.3 Electricity Sale Prices

According to the Turkish Law No.5346, solar and biomass power plants that have come into operation since 18 May 2005 or will come into operation before 31 December 2020, will be eligible to receive 133 $/MWh feed-in tariff of the first ten years of their operation.

For the remaining financial period, electricity price forecast of commercial companies has been taken into consideration. Electricity sales price used in the financial model are given in Table 13 below.

Table 13 Electricity Sales Price Used in the Financial Model

Year	Sales Price ($/kWh)	Year	Sales Price ($/kWh)
2028	0.083	2035	0.085
2029	0.084	2036	0.086
2030	0.084	2037	0.088
2031	0.084	2038	0.089
2032	0.084	2039	0.090
2033	0.085	2040	0.092
2034	0.085	2041	0.093

5.4 Capital Expenditures (CAPEX)

CAPEX represents the total expenditure required to achieve commercial operation in a given year. Capital Expenditures consist of the development cost, land cost, equipment cost (solar collectors, solar receiver, piping, heat transfer fluid system, biomass boiler, steam turbine, cooling system, pumps and power block), construction, electrical infrastructure and commissioning costs. CAPEX may not explicitly represent regional variants associated with labor rates, material costs, etc. or geographically determined spur lines costs.

Unit Capital Expenditure ($/kW) values, excluding land cost, are taken from Transparent Cost Database which is prepared by National Renewable Energy Laboratory (NREL)[61]. The database includes capital cost, operation & maintenance (O&M) cost, utility scale capacity factors, useful life of the technology and land use by system technology for distributed generation systems. For utility scale technologies, the database includes capital cost, variable and fixed O&M cost and capacity factors for selected technologies. Unit Capital Cost for selected electricity generation technologies are given in Figure 34.

Unit Capital Cost for CSP technology is 6,290 $/kW and cost of solar collectors and HTF system is ~40% of this price. Power unit, steam turbine and balance of plant will be in common with the biomass part. Therefore, unit CAPEX for solar part is assumed as 2,516 $/kW. Regarding the biomass fired power plant, unit capital cost is 3,370 $/kW. Thus, overall capital cost excluding land cost is calculated as 5,886 $/kW.

Required land size for CSP technology is 13.2 m^2/kW (774 Btu/ft^2-day) and for biomass combustion systems it is 14.2 m^2/kW (3.5 acres/MW) [62]. So, the total area required for the proposed hybrid system is 27.4 m^2/kW. Considering land prices in Kırklareli region (~2.75 $/$m^2$), unit land cost is found as 75,273 $/MW. Therefore, overall capital cost including land cost is calculated as 5,961 $/kW.

Total CAPEX including land cost is calculated as $5.96 M for 1 MW installed capacity and $29.81 M for 5 MW installed capacity.

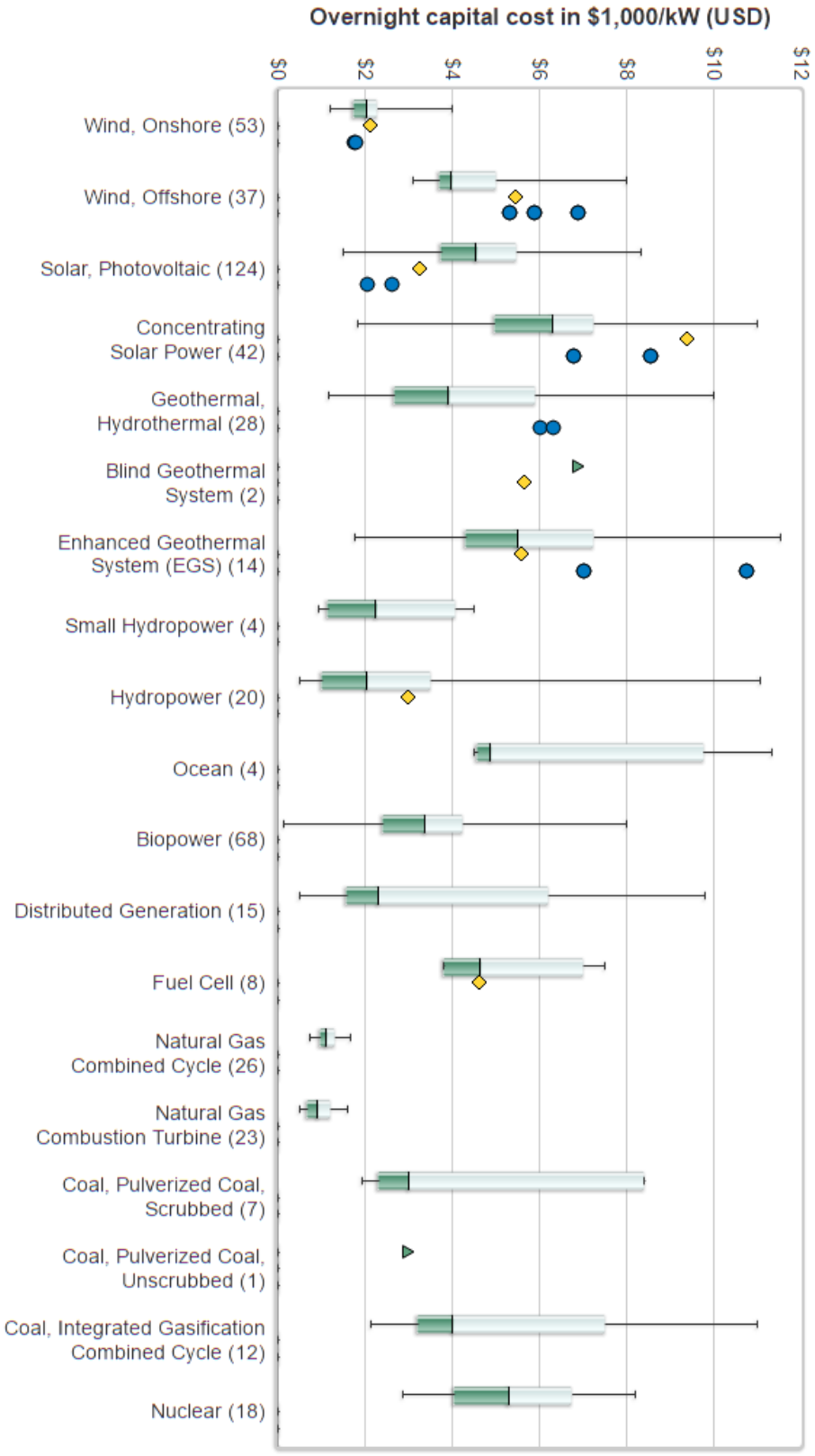

Figure 34 Capital Cost of Selected Electricity Generation Technologies [61]

5.5 Operational Expenditures (OPEX)

Operating costs for power plants include fuel, labor and maintenance costs. Unlike capital costs which are "fixed", i.e. do not vary with the level of output, total operating cost depends on the total amount of electricity produced in the power plant.

Figure 35 shows unit fixed operating costs of selected electricity generation technologies. Unit fixed operating cost for CSP technology is 65.0 $/kW and for biomass fired power plant is 99.4$/kW. Assuming 40% of the fixed cost will be caused by common facilities, fixed operating cost for solar part can be taken as 26.00 $/kW. Total fixed operating cost for the hybrid system is found as 125.4 $/kW. Fixed operating cost for 1 MW installed capacity is calculated as $125,400 and $627,000 for 5 MW installed capacity.

Unit variable operating cost of selected electricity generation technologies is indicated in Figure 36. Unit variable operating cost for CSP technology is 3.0 $/MWh and for biomass fired power plant is 4.2 $/kW. Assuming 40% of the ariable cost will be caused by common facilities, variable operating cost for solar part can be taken as 1.2 $/MWh. Total variable operating cost for the hybrid system is found as 5.4 $/MWh. Considering the total annual generation amounts explained in Section 5.2, annual variable operating cost is $39,735 for 1 MW and $198,677 for 5 MW installed capacity. Variable and Fixed unit operating cost values are escalated by US CPI for the future years.

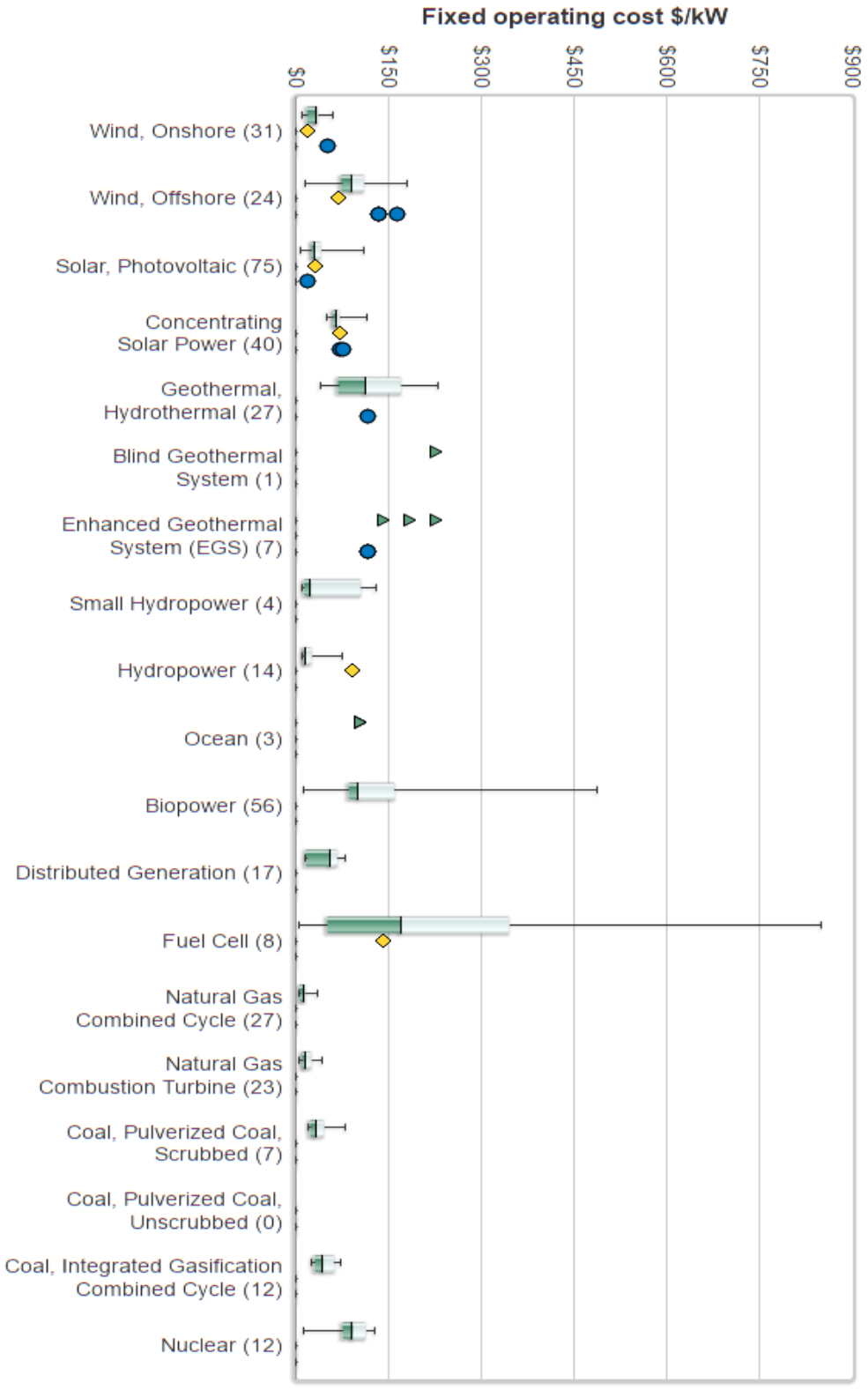

Figure 35 Fixed Operating Cost of Selected Electricity Generation Technologies [61]

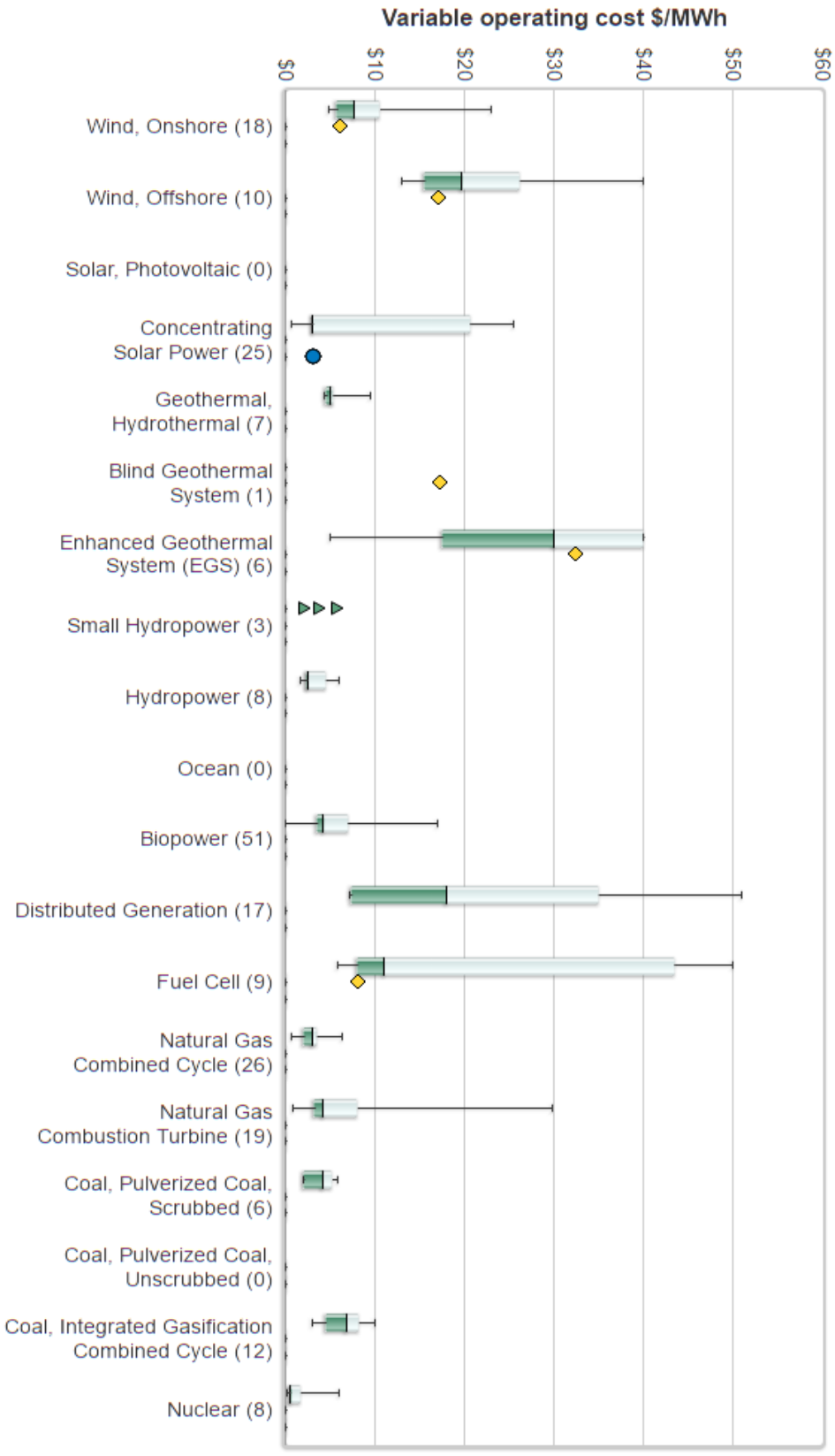

Figure 36 Variable Operating Cost of Selected Electricity Generation Technologies [61]

Calculated Generation, CAPEX and OPEX values for 1 MW and 5 MW installed capacity are shown in Table 14.

Table 14 Generation, CAPEX and OPEX for 1MW and 5MW Installed Capacities

	1 MW	**5 MW**
Generation	7’358 MWh/year	36’792 MWh/year
CAPEX	$5,961,273	$29,806,365
OPEX	$165,135	$825,677
Fixed	$125,400	$627,000
Variable	$39,735	$198,677

5.6 Financing Alternatives

Two financing alternatives that investors could use to finance the initial investment cost of the hybrid system were assessed. These alternatives are:

I. 100% Equity: All the initial investment cost is covered by the equity capital. (0% Debt: 100% Equity)
II. 20% Equity: 20% of the initial investment cost is covered by the equity capital, 80% is covered by the loan. (80% Debt: 20% Equity).

For the second case, credit tenor is taken as 10 years which is equal to feed-in-tariff period. Interest rate is assumed as 3.5%.

5.7 Cash Flows

Cash flow statements for each financing alternative have been prepared to show the future cash inflows and the cash outflows. Cash flow statement for 100% equity financing is shown in Table 15 for 1 MW and in Table 16 for 5 MW.
Cash flow statement for 20% equity financing is shown in Table 17 for 1 MW and in Table 18 for 5 MW.

Table 15 Cash Flow Statement for 100% Equity Financing (1 MW)

	Cash Inflow	**Cash Outflow**				**Net CF**	**Cum. Net Project CF**
	Revenue	OPEX	Interest Payment	Cor. Tax Payment	Principal Payment	Project CF	
0	$0	$0	$0	$0	$0	-$5,961,273	-$5,961,273
1	$978,667	$165,135	$0	$43,481	$0	$770,051	-$5,191,222
2	$978,667	$168,603	$0	$45,291	$0	$764,773	-$4,426,449
3	$978,667	$172,144	$0	$47,034	$0	$759,489	-$3,666,960
4	$978,667	$175,759	$0	$48,711	$0	$754,198	-$2,912,762
5	$978,667	$179,450	$0	$50,322	$0	$748,895	-$2,163,867
6	$978,667	$183,218	$0	$51,868	$0	$743,581	-$1,420,286
7	$978,667	$187,066	$0	$53,350	$0	$738,251	-$682,035
8	$978,667	$190,994	$0	$54,769	$0	$732,904	$50,869
9	$978,667	$195,005	$0	$56,125	$0	$727,537	$778,406
10	$978,667	$199,100	$0	$57,419	$0	$722,148	$1,500,555
11	$611,483	$203,281	$0	$81,640	$0	$326,561	$1,827,116
12	$614,426	$207,550	$0	$81,375	$0	$325,501	$2,152,617
13	$616,634	$211,909	$0	$80,945	$0	$323,780	$2,476,397
14	$618,841	$216,359	$0	$80,497	$0	$321,986	$2,798,383
15	$620,313	$220,902	$0	$79,882	$0	$319,529	$3,117,912
16	$622,521	$225,541	$0	$79,396	$0	$317,583	$3,435,495
17	$624,728	$230,278	$0	$78,890	$0	$315,560	$3,751,055
18	$626,936	$235,114	$0	$78,364	$0	$313,458	$4,064,513
19	$636,340	$240,051	$0	$79,258	$0	$317,031	$4,381,544
20	$645,885	$245,092	$0	$80,159	$0	$320,634	$4,702,178
21	$655,573	$250,239	$0	$81,067	$0	$324,267	$5,026,446
22	$665,407	$255,494	$0	$81,983	$0	$327,930	$5,354,376
23	$675,388	$260,859	$0	$82,906	$0	$331,623	$5,685,998
24	$685,519	$266,337	$0	$83,836	$0	$335,345	$6,021,343
25	$694,916	$271,930	$0	$84,597	$0	$338,389	$6,359,732

Table 16 Cash Flow Statement for 100% Equity Financing (5 MW)

	Cash Inflow	**Cash Outflow**				**Net CF**	**Cum. Net Project CF**
	Revenue	OPEX	Interest Payment	Cor. Tax Payment	Principal Payment	Project CF	
0	$0	$0	$0	$0	$0	-$29,806,365	-$29,806,365
1	$4,893,336	$825,677	$0	$217,405	$0	$3,850,255	-$25,956,110
2	$4,893,336	$843,016	$0	$226,455	$0	$3,823,865	-$22,132,246
3	$4,893,336	$860,719	$0	$235,170	$0	$3,797,446	-$18,334,800
4	$4,893,336	$878,794	$0	$243,554	$0	$3,770,988	-$14,563,812
5	$4,893,336	$897,249	$0	$251,609	$0	$3,744,477	-$10,819,334
6	$4,893,336	$916,091	$0	$259,341	$0	$3,717,904	-$7,101,430
7	$4,893,336	$935,329	$0	$266,751	$0	$3,691,255	-$3,410,175
8	$4,893,336	$954,971	$0	$273,845	$0	$3,664,520	$254,345
9	$4,893,336	$975,026	$0	$280,624	$0	$3,637,686	$3,892,031
10	$4,893,336	$995,501	$0	$287,093	$0	$3,610,742	$7,502,773
11	$3,057,415	$1,016,407	$0	$408,202	$0	$1,632,807	$9,135,579
12	$3,072,132	$1,037,751	$0	$406,876	$0	$1,627,505	$10,763,084
13	$3,083,170	$1,059,544	$0	$404,725	$0	$1,618,900	$12,381,985
14	$3,094,207	$1,081,794	$0	$402,483	$0	$1,609,930	$13,991,915
15	$3,101,566	$1,104,512	$0	$399,411	$0	$1,597,643	$15,589,558
16	$3,112,603	$1,127,707	$0	$396,979	$0	$1,587,917	$17,177,475
17	$3,123,641	$1,151,389	$0	$394,450	$0	$1,577,802	$18,755,276
18	$3,134,678	$1,175,568	$0	$391,822	$0	$1,567,288	$20,322,565
19	$3,181,699	$1,200,255	$0	$396,289	$0	$1,585,155	$21,907,720
20	$3,229,424	$1,225,460	$0	$400,793	$0	$1,603,171	$23,510,891
21	$3,277,865	$1,251,195	$0	$405,334	$0	$1,621,337	$25,132,228
22	$3,327,033	$1,277,470	$0	$409,913	$0	$1,639,651	$26,771,878
23	$3,376,939	$1,304,297	$0	$414,528	$0	$1,658,114	$28,429,992
24	$3,427,593	$1,331,687	$0	$419,181	$0	$1,676,725	$30,106,717
25	$3,474,581	$1,359,652	$0	$422,986	$0	$1,691,943	$31,798,660

Table 17 Cash Flow Statement for 20% Equity Financing (1 MW)

	Cash Inflow	**Cash Outflow**				**Net CF**	**Cum. Net Project CF**
	Revenue	OPEX	Interest Payment	Cor. Tax Payment	Principal Payment	Project CF	
0	$0	$0	$0	$0	$0	-$1,192,255	-$1,192,255
1	$978,667	$165,135	$175,261	$8,429	$476,902	$152,940	-$1,039,315
2	$978,667	$168,603	$157,735	$13,744	$476,902	$161,683	-$877,632
3	$978,667	$172,144	$140,209	$18,992	$476,902	$170,420	-$707,212
4	$978,667	$175,759	$122,683	$24,174	$476,902	$179,149	-$528,062
5	$978,667	$179,450	$105,157	$29,291	$476,902	$187,868	-$340,194
6	$978,667	$183,218	$87,631	$34,342	$476,902	$196,574	-$143,620
7	$978,667	$187,066	$70,105	$39,329	$476,902	$205,266	$61,646
8	$978,667	$190,994	$52,578	$44,253	$476,902	$213,939	$275,585
9	$978,667	$195,005	$35,052	$49,114	$476,902	$222,594	$498,179
10	$978,667	$199,100	$17,526	$53,913	$476,902	$231,226	$729,404
11	$611,483	$203,281	$0	$81,640	$0	$326,561	$1,055,966
12	$614,426	$207,550	$0	$81,375	$0	$325,501	$1,381,467
13	$616,634	$211,909	$0	$80,945	$0	$323,780	$1,705,247
14	$618,841	$216,359	$0	$80,497	$0	$321,986	$2,027,233
15	$620,313	$220,902	$0	$79,882	$0	$319,529	$2,346,761
16	$622,521	$225,541	$0	$79,396	$0	$317,583	$2,664,345
17	$624,728	$230,278	$0	$78,890	$0	$315,560	$2,979,905
18	$626,936	$235,114	$0	$78,364	$0	$313,458	$3,293,363
19	$636,340	$240,051	$0	$79,258	$0	$317,031	$3,610,394
20	$645,885	$245,092	$0	$80,159	$0	$320,634	$3,931,028
21	$655,573	$250,239	$0	$81,067	$0	$324,267	$4,255,295
22	$665,407	$255,494	$0	$81,983	$0	$327,930	$4,583,225
23	$675,388	$260,859	$0	$82,906	$0	$331,623	$4,914,848
24	$685,519	$266,337	$0	$83,836	$0	$335,345	$5,250,193
25	$694,916	$271,930	$0	$84,597	$0	$338,389	$5,588,582

Table 18 Cash Flow Statement for 20% Equity Financing (5 MW)

	Cash Inflow	**Cash Outflow**				**Net CF**	**Cum. Net Project CF**
	Revenue	OPEX	Interest Payment	Cor. Tax Payment	Principal Payment	Project CF	
0	$0	$0	$0	$0	$0	-$5,961,273	-$5,961,273
1	$4,893,336	$825,677	$876,307	$42,143	$2,384,509	$764,700	-$5,196,573
2	$4,893,336	$843,016	$788,676	$68,720	$2,384,509	$808,414	-$4,388,159
3	$4,893,336	$860,719	$701,046	$94,961	$2,384,509	$852,100	-$3,536,059
4	$4,893,336	$878,794	$613,415	$120,871	$2,384,509	$895,746	-$2,640,312
5	$4,893,336	$897,249	$525,784	$146,453	$2,384,509	$939,341	-$1,700,971
6	$4,893,336	$916,091	$438,154	$171,710	$2,384,509	$982,872	-$718,099
7	$4,893,336	$935,329	$350,523	$196,647	$2,384,509	$1,026,328	$308,229
8	$4,893,336	$954,971	$262,892	$221,266	$2,384,509	$1,069,697	$1,377,926
9	$4,893,336	$975,026	$175,261	$245,572	$2,384,509	$1,112,968	$2,490,893
10	$4,893,336	$995,501	$87,631	$269,567	$2,384,509	$1,156,128	$3,647,021
11	$3,057,415	$1,016,407	$0	$408,202	$0	$1,632,807	$5,279,828
12	$3,072,132	$1,037,751	$0	$406,876	$0	$1,627,505	$6,907,333
13	$3,083,170	$1,059,544	$0	$404,725	$0	$1,618,900	$8,526,233
14	$3,094,207	$1,081,794	$0	$402,483	$0	$1,609,930	$10,136,163
15	$3,101,566	$1,104,512	$0	$399,411	$0	$1,597,643	$11,733,806
16	$3,112,603	$1,127,707	$0	$396,979	$0	$1,587,917	$13,321,723
17	$3,123,641	$1,151,389	$0	$394,450	$0	$1,577,802	$14,899,525
18	$3,134,678	$1,175,568	$0	$391,822	$0	$1,567,288	$16,466,814
19	$3,181,699	$1,200,255	$0	$396,289	$0	$1,585,155	$18,051,969
20	$3,229,424	$1,225,460	$0	$400,793	$0	$1,603,171	$19,655,140
21	$3,277,865	$1,251,195	$0	$405,334	$0	$1,621,337	$21,276,476
22	$3,327,033	$1,277,470	$0	$409,913	$0	$1,639,651	$22,916,127
23	$3,376,939	$1,304,297	$0	$414,528	$0	$1,658,114	$24,574,241
24	$3,427,593	$1,331,687	$0	$419,181	$0	$1,676,725	$26,250,966
25	$3,474,581	$1,359,652	$0	$422,986	$0	$1,691,943	$27,942,908

5.8 Evaluation Criteria

Two basic financial criteria have been considered in the financial evaluation of proposed hybrid system. These are the basic criteria that are widely used in the evaluation of investment projects and in making investment decisions.

a. Net Present Value (NPV): NPV is the difference between the present value of cash inflows and the present value of cash outflows throughout the economic life of the project. A positive NPV indicates the investment will be profitable whereas a negative NPV will result in a net loss.
b. Internal Rate of Return (IRR): IRR is the discount ratio which makes NPV of all cash flows through economic life of the project equal to zero. IRR is used to measure profitability of potential investments. The higher IRR of a project, the more desirable it is to undertake the project.

5.9 Financial Analysis Results

NPV and IRR values have been calculated for all financing alternatives and installed capacities. Results are given in Table 19.

Table 19 Financial Analysis Results

Financing Alternative	Installed Capacity	NPV	IRR
100% Equity	1 MW	-$403,912	5.50%
	5 MW	-$2,019,558	5.50%
20% Equity	1 MW	$894,184	15.64%
	5 MW	$4,470,922	15.64%

CHAPTER 6

DISCUSSION & CONCLUSION

6.1 Summary

In this study; simulation models for 1 MW_e and 5 MW_e Rankine cycle based solar-biomass hybrid power plants were developed using the ASPEN PLUS software and a financial analysis was conducted via MS EXCEL. Using the simulation model; thermal efficiency, fuel consumption rate, CO2 emissions were investigated for both installed capacities.

During the simulations, two alternatives (CASE-I and CASE-II) were investigated to obtain a constant steam temperature at the turbine inlet since the thermodynamic properties of the HTF do not allow the steam temperature to be increased up to 530°C. CASE-I considers an auxiliary methane fired boiler which superheats the steam coming from solar collectors. For CASE-II, a biomass boiler is also considered for superheating the solar steam and connected in parallel to the solar part. Simulation results are shown in Table 20.

In the financial analysis, only CASE-II has been taken into consideration and an evaluation has been made using different financial parameters. Net Present Value (NPV) and Internal Rate of Return (IRR) have been calculated for both 1 MW and 5 MW installed capacities. During calculations 100% equity and 20% equity financing models are considered.

Table 20 Summary of the Results

		1 MW	5 MW
CASE –I	Biomass Consumption	9,012 ton	51,127 ton
	CH_4 Consumption	70,857 m^3	340,749 m^3
	CO_2 Emission	13,009 ton	72,691 ton
	Thermal Efficiency	14.39%	14.43%
CASE –II	Biomass Consumption	9,157 ton	51,490 ton
	CO_2 Emission	12,911 ton	72,601 ton
	Thermal Efficiency	14.35%	14.49%

6.2 Discussion & Conclusion

The study shows that hybridization decreases biomass consumption and CO_2 emissions. In CASE-I, CO_2 emissions released by the methane boiler have been calculated as 302 tons/year for 1 MW and total emission is 13,009 tons/year. In CASE-II, total emissions are lower and equal to 12,911 tons/year. Therefore, in terms of CO_2 emission, CASE-II is preferable than CASE-I since hybridizing solar collectors directly with biomass boiler decreases CO_2 emissions by 0.8%.

Moreover, the results are compared to biomass only power plant with the same installed capacity. The assessment shows that hybridizing biomass with solar energy reduces the biomass consumption by 18%. In addition, annual CO_2 emissions of the biomass only system are 20% higher compared to the hybrid system.

Negative NVP values indicated that the investment as 100% equity will result in an overall loss at the end of the financial period which makes the project not suitable for investment. It is seen from the financial analysis that NPV values of both 1 MW and 5 MW projects are negative for 100% equity financing. On the other hand, renewable energy projects are founded and supported by all the financial institutions and it can

be easily financed with 80:20 debt to equity ratio since the project is able to benefit from Feed-in-Tariff with a high sales prices for 10 years. NPV values for both 1 MW and 5 MW projects are positive for 20% equity financing. Furthermore, IRR is 15.64% which is above the current interest rates in Turkey that makes the project feasible for investment.

All in all, continuous electricity generation with solar only systems is not possible without storage; therefore the proposed solar-biomass hybrid solution not only provides continuous electricity generation but also reduces the consumption of biomass. Consequently, the hybrid system lowers the carbon footprint by burning less biomass. Moreover, the required investment cost and O&M costs are not too high compared to the standalone systems since most of the facilities such as steam turbine and power electronics are common for both systems. Hence, the solar-biomass hybrid plant is feasible also in term of economics. It is important to obtain an alternative solution to reduce the use of fossil based thermal power plants and their CO_2 footprint and hybrid power plants seem to be appropriate solutions both in terms of continuous power generation and emissions reduction.

6.3 Future Works

As for the future works, the simulation model can be run for different values for the Turbine Inlet Pressure and Temperature and the Solar Collector Area. In addition that the number of turbine stages can also be changed and different pressure levels (HP, MP and LP) can be considered. Moreover, various biomass types can be used for the biomass boiler and different fuels (i.e. natural gas, biomass) can be used in the auxiliary boiler.

REFERENCES

[1] "World Energy Statistical Year Book," 2017. [Online]. Available: https://yearbook.enerdata.net/. [Accessed: 16-Sep-2017].

[2] Y. Sonu, L. H. Devred, L. E. N. S. Yap, L. E. T. S. Yap, L. E. T. Devret, S. Serbest, S. Santraller, T. Kurulu, K. Mw, K. Mw, Y. Sonu, O. K. Y. Kati, O. K. Y. Sivi, G. A. Z. Jeotermal, and K. Mw, "Türkiye elektrik sistemi kuruluş ve yakit cinslerine göre kurulu güç 2017," 2017.

[3] "The Law on Utilization of Renewable Energy Resources of the Purpose of Generating Electrical Energy No. 5346." .

[4] "Greenway CSP Solar Tower." [Online]. Available: http://www.greenwaycsp.com/en/field-applications/mersin-5-mwth-solar-tower-plant.aspx. [Accessed: 25-Aug-2017].

[5] "TEİAŞ, Turkish Electicity Transmission Company," 2017. [Online]. Available: www.teias.gov.tr/yukdagitim/kuruluguc.xls.

[6] "General Directorate of Renewable Energy." [Online]. Available: http://www.eie.gov.tr/MyCalculator/Default.aspx. [Accessed: 25-May-2017].

[7] "General Directorate of Renewable Energy." [Online]. Available: http://bepa.yegm.gov.tr/. [Accessed: 25-Aug-2017].

[8] A. Fernández-García, E. Zarza, L. Valenzuela, and M. Pérez, "Parabolic-trough solar collectors and their applications," *Renew. Sustain. Energy Rev.*, vol. 14, no. 7, pp. 1695–1721, 2010.

[9] H. Müller-Steinhagen and F. Trieb, "Concentrating solar power - A review of the technology," *Q. R. Acad. Eng.*, pp. 43–50, 2004.

[10] D. Barlev, R. Vidu, and P. Stroeve, "Innovation in concentrated solar power," *Sol. Energy Mater. Sol. Cells*, vol. 95, no. 10, pp. 2703–2725, 2011.

[11] S. Kalogirou, *Solar Energy Engineering*. 2009.

[12] "Alternative Energy Tutorials," 2015. [Online]. Available: http://www.alternative-energy-tutorials.com/solar-hot-water/parabolic-trough-reflector.html. [Accessed: 25-Aug-2017].

[13] T. M. Pavlović, I. S. Radonjić, D. D. Milosavljević, and L. S. Pantić, "A review of concentrating solar power plants in the world and their potential use in Serbia," *Renew. Sustain. Energy Rev.*, vol. 16, no. 6, pp. 3891–3902, 2012.

[14] P. McKendry, "Energy production from biomass (part 2): Conversion technologies," *Bioresour. Technol.*, vol. 83, no. 1, pp. 47–54, 2002.

[15] P. Quaak, H. Knoef, and H. Stassen, "Energy from Biomass a review of

combustion and gasification technologies," *World Bank Tech. Pap.*, no. 422, pp. 1–78, 1999.

[16] J. Koppejan and S. van Loo, *The Handbook of Biomass Combustion and Co-firing*. 2008.

[17] A. Faaij, *Modern Biomass Conversion Technologies*, vol. 11, no. 2. 2006.

[18] S. C. Campareda, "Biomass Energy Conversion," *Sustain. Growth Appl. Renew. Energy Sources*, no. 2, 2011.

[19] G. Lorenzini, C. Biserni, and G. Flacco, *Solar Thermal and Biomass Energy*, vol. 32. 2010.

[20] M. Zekiyilmazoglu, A. Durmaz, and D. Baker, "Solar repowering of Soma-A thermal power plant," *Energy Convers. Manag.*, vol. 64, pp. 232–237, 2012.

[21] "TYT Energy - Gümüşköy GPP." [Online]. Available: http://www.tyt.com.tr/tr/geosolar/overview#. [Accessed: 25-Aug-2017].

[22] O. C. Kuyumcu, U. Z. D. Solarglu, S. Akar, and O. Serin, "Hybrid Geothermal and Solar Thermal Power Plant Case Study: Gumuskoy GEPP," *GHC Bull.*, vol. 36, 2013.

[23] A. Turan, "Assessment of Geothermal and Solar Hybrid Power Generation Technologies in Turkey and Its Application to Menderes Graben," *World Geotherm. Congr. 2015*, no. April, pp. 19–25, 2015.

[24] S. Solmaz and A. Turan, "Ortalama Geçmiş Rüzgar Verileri Üzerinden Rüzgar Enerjisi Santralleri için Ön Fizibilite Yapılması : Gediz Üniversitesi 100 kW Rüzgar Enerjisi Uygulaması," 2015, pp. 71–85.

[25] S. Solmaz, "GEDİZ ÜNİVERSİTESİ HİBRİT ENERJİ SANTRALİ ve 100 kW RÜZGAR TÜRBİNİ UYGULAMASI." 2015.

[26] D. Morell, "CSP BORGES The World's First CSP plant hybridized with biomass," *CSP Today USA 2012 - 6th Conc. Sol. Therm. Power Conf.*, no. June, 2012.

[27] a Cot, a Amettler, J. Vall-Llovera, J. Aguilo, and J. M. Arque, "Termosolar Borges: A Thermosolar Hybrid Plant with Biomass," *Third Int. Symp. Energy from Biomass Waste*, no. November, 2010.

[28] "Falck Renewables." [Online]. Available: http://www.falckrenewables.eu/~/media/Files/F/Falck-Renewables-Bm2012/pdfs/press-release/2014/FKR Press release_SolareTermodinamico.pdf. [Accessed: 25-Aug-2017].

[29] "Thermosolar Borges." [Online]. Available: https://en.wikipedia.org/wiki/Termosolar_Borges. [Accessed: 25-May-2017].

[30] N. B. Desai, S. Bandyopadhyay, J. K. Nayak, R. Banerjee, and S. B. Kedare, "Simulation of 1MWe Solar Thermal Power Plant," *Energy Procedia*, vol. 57, no. 2012, pp. 507–516, 2014.

[31] T. Srinivas and B. V. Reddy, “Hybrid solar-biomass power plant without energy storage,” *Case Stud. Therm. Eng.*, vol. 2, pp. 75–81, 2014.

[32] J. D. Nixon, P. K. Dey, and P. a. Davies, “The feasibility of hybrid solar-biomass power plants in India,” *Energy*, vol. 46, no. 1, pp. 541–554, 2012.

[33] J. Nixon and J. D. Nixon, “Solar thermal collectors for use in hybrid solar-biomass power plants in India power plants in India,” Aston University, 2012.

[34] J. Servert, G. San Miguel, and D. López, “Hybrid solar - Biomass plants for power generation; technical and economic assessment,” *Glob. Nest J.*, vol. 13, no. 3, pp. 266–276, 2011.

[35] J. H. Peterseim, S. White, A. Tadros, and U. Hellwig, “Concentrated solar power hybrid plants, which technologies are best suited for hybridisation?,” *Renew. Energy*, vol. 57, pp. 520–532, 2013.

[36] J. H. Peterseim, U. Hellwig, A. Tadros, and S. White, “Hybridisation optimization of concentrating solar thermal and biomass power generation facilities,” *Sol. Energy*, vol. 99, pp. 203–214, 2014.

[37] J. H. Peterseim, S. White, A. Tadros, and U. Hellwig, “Concentrating solar power hybrid plants - Enabling cost effective synergies,” *Renew. Energy*, vol. 67, pp. 178–185, 2014.

[38] J. H. Peterseim, a. Tadros, S. White, U. Hellwig, J. Landler, and K. Galang, “Solar tower-biomass hybrid plants - Maximizing plant performance,” *Energy Procedia*, vol. 49, no. 0, pp. 1197–1206, 2013.

[39] Z. Bai, Q. Liu, J. Lei, X. Wang, J. Sun, and H. Jin, “Thermodynamic evaluation of a novel solar-biomass hybrid power generation system,” *Energy Convers. Manag.*, vol. 142, pp. 296–306, 2017.

[40] C. M. I. Hussain, B. Norton, and A. Duffy, “Technological assessment of different solar-biomass systems for hybrid power generation in Europe,” *Renew. Sustain. Energy Rev.*, vol. 68, pp. 1115–1129, 2017.

[41] M. Ouagued, A. Khellaf, and L. Loukarfi, “Estimation of the temperature, heat gain and heat loss by solar parabolic trough collector under Algerian climate using different thermal oils,” *Energy Convers. Manag.*, vol. 75, pp. 191–201, 2013.

[42] P. Selvakumar, S. Prasanth, N. Rakesh, and A. Vignesh, “Fluid flow and heat transfer analysis on multiple parabolic trough collectors by varying heat transfer fluids,” Anna University of Technology Coimbatore, 2011.

[43] P. Selvakumar, P. Somasundaram, and P. Thangavel, “Performance study on evacuated tube solar collector using therminol D-12 as heat transfer fluid coupled with parabolic trough,” *Energy Convers. Manag.*, vol. 85, pp. 505–510, 2014.

[44] “Therminol® Heat Transfer Fluids.” [Online]. Available:

https://www.therminol.com/products. [Accessed: 25-Aug-2017].

[45] M. Biencinto, L. Gonzalez, E. Zarza, L. E. Diez, and J. Munoz-Anton, "Performance model and annual yield comparison of parabolic-trough solar thermal power plants with either nitrogen or synthetic oil as heat transfer fluid," *Energy Convers. Manag.*, vol. 87, pp. 238–249, 2014.

[46] M. J. Montes, A. Abanades, J. M. Martinez-Val, and M. Valdes, "Solar multiple optimization for a solar-only thermal power plant, using oil as heat transfer fluid in the parabolic trough collectors," *Sol. Energy*, vol. 83, no. 12, pp. 2165–2176, 2009.

[47] A. Fontalvo, J. Garcia, M. Sanjuan, and R. V. Padilla, "Automatic control strategies for hybrid solar-fossil fuel power plants," *Renew. Energy*, vol. 62, pp. 424–431, 2014.

[48] M. J. Moran and H. N. Shapiro, *Fundamentals of Engineering Thermodynamics*. 2006.

[49] "Photovoltaic Geographical Information System (PVGIS)," 2017. [Online]. Available: http://re.jrc.ec.europa.eu/pvgis/. [Accessed: 16-Sep-2017].

[50] A. Giostri, M. Binotti, M. Astolfi, P. Silva, E. Macchi, and G. Manzolini, "Comparison of different solar plants based on parabolic trough technology," *Sol. Energy*, vol. 86, no. 5, pp. 1208–1221, 2012.

[51] G. Manzolini, A. Giostri, C. Saccilotto, P. Silva, and E. Macchi, "Development of an innovative code for the design of thermodynamic solar power plants part B: Performance assessment of commercial and innovative technologies," *Renew. Energy*, vol. 36, no. 9, pp. 2465–2473, 2011.

[52] M. L. Sweet and J. T. McLeskey, "Numerical simulation of underground Seasonal Solar Thermal Energy Storage (SSTES) for a single family dwelling using TRNSYS," *Sol. Energy*, vol. 86, no. 1, pp. 289–300, 2012.

[53] R. Schefflan, *Teach yourself the basics of ASPEN PLUS*, vol. 1. John Wiley & Sons, Inc., 2011.

[54] C. Telmo, J. Lousada, and N. Moreira, "Proximate analysis, backwards stepwise regression between gross calorific value, ultimate and chemical analysis of wood," *Bioresour. Technol.*, vol. 101, no. 11, pp. 3808–3815, 2010.

[55] D. J. Bushnell, "Bıomass Fuel Charecterization: Testing and Evaluating the Combustion Characteristics of Selected Bıomass Fuels," Oregon State University, 1989.

[56] M. Hellwig, "Energy from Biomass 3rd. E.C. Conference," in *Basic of the Combustion of Wood and Straw*, 1985, pp. 891–896.

[57] Siemens, "Pre-designed Steam Turbines," p. 8, 2013.

[58] BLS, "CPI Detailed Report Data for December 2015," 2015.

[59] Gelir İdaresi Başkanlığı, "Kurumlar Vergisi Oranlari." [Online]. Available:

http://www.gib.gov.tr/fileadmin/user_upload/Yararli_Bilgiler/KV_Oranlari.html. [Accessed: 22-Jul-2017].

[60] "Amortismana Tabi İktisadi Kıymetler Faydalı Ömür (Yıl) Normal Amortisman Oranı İlgili Genel Tebliğ."

[61] National Renewable Energy Laboratory (NREL), "Transparent Cost Database | Transparent Cost Database." [Online]. Available: http://en.openei.org/apps/TCDB/#blank. [Accessed: 22-Jul-2017].

[62] National Renewable Energy Laboratory (NREL), "Land Use by System Technology." [Online]. Available: http://www.nrel.gov/analysis/tech_size.html. [Accessed: 22-Jul-2017].

APPENDICES

APPENDIX A

User Manuel for Aspen Plus

1) Solar Field

The block diagram indicating the solar field is given in Figure 37. “Calculator” block (“DNIVALUE”) is used to convert the direct normal irradiance values to thermal energy amount received by the collectors. “FSplit” block (“LOSS”) is inserted to simulate the heat loss to the surrounding. “QSOLAR” is the heat stream between sun and collector surface. “QLOSS” stands for the heat loss to surrounding whereas “QIN” represents the heat flow to the HTF from the collector surface.

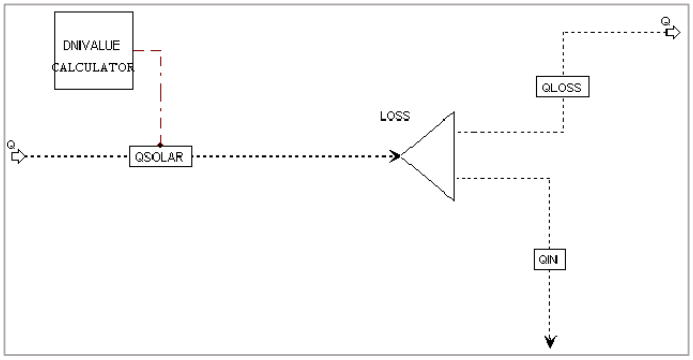

Figure 37 Block Diagram of Solar Solar Collectors

Figure 38 indicates the heat transfer process between oil (Therminol VP-1) and water. To be on the safe side, inlet temperature of Therminol VP-1 (“OIL-IN”) is determined as 290°C with a pressure of 10 bar and it is heated up to 390°C. It is assumed that the oil is operating at constant pressure in closed cycle and no heat and material losses. Therefore, temperature of oil exit stream (“OIL-OUT”) is set to 290°C.

"Heater" block ("SOL-HEX") is used to model the heat transfer process between the collectors and HTF. The heat exchanger is modelled with 2 "Heater" blocks ("SOL-EVAP") and a heat stream ("QOIL") to connect them [53].

"WATER-IN" is stands for the inlet water stream to the heat exchanger and it is at 25°C (ambient temperature), 40 bar (turbine inlet pressure). Phase change occurs in the heat exchanger. Thus, the water leaves the heat exchanger ("SOL-VAP") in vapor phase at 389°C and 40 bar.

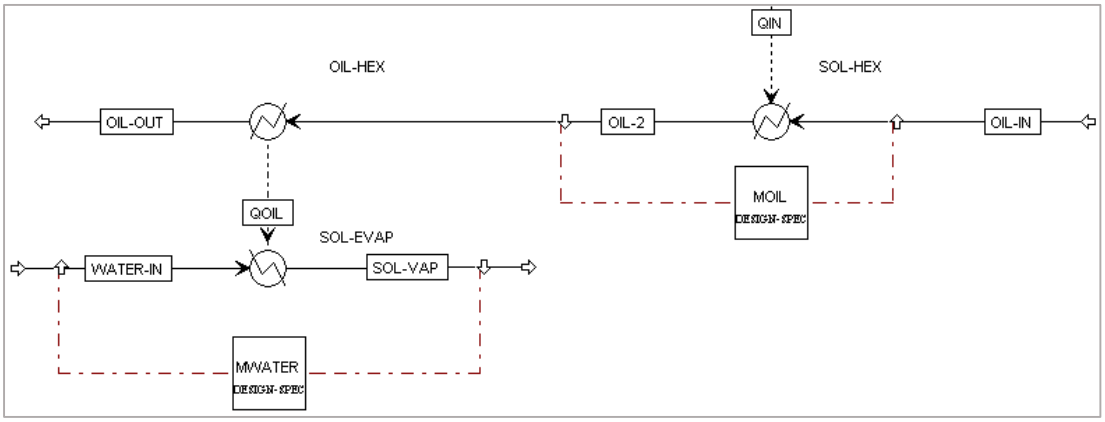

Figure 38 Block Diagram Showing Heat Transfer between HTF and Water

Control strategies can be simulated by a "Design-Spec" block. "MOIL" (Figure 38) manipulates the flow rate of oil according to the variations in DNI values so that the collector exit temperature is kept below 390°C with a tolerance of 0,1°C. Mass flow rate of inlet water is manipulated by "MWATER" to obtain vapor at 389°C at the exit of the collector.

2) Biomass Boiler

Biomass is modelled as a non-conventional solid fuel in ASPEN PLUS. First, stream class in global settings should be selected as "MCINCPSD" to be able to work with solid materials like carbon, ash and biomass. Biomass fuel and ash should be specified as non-conventional material. "HCOALGEN" and "DCOALIGT" are used as the Property Method to calculate the enthalpy and density of solid material. "HCOALGEN" uses the proximate analysis, ultimate analysis and sulfur analysis to

calculate the enthalpy of material. Heat of combustion value for the non-conventional fuel (“HCOMB”) and other input values for Proxanal, Ultanal and Sulfanal attributes should be entered to define the fuel. Ultimate and Proximate analysis for the selected biomass is given in Section 3.

Block diagram simulating the direct combustion process of biomass is shown in Figure 39. After completion of above mentioned inputs, “BIOMASS” stream shown in Figure 39 is defined. The other inlet stream is “AIR” which indicates the air input to the combustion chamber. It is assumed that the air is at atmospheric pressure (1 bar) and ambient temperature (15°C). Mole fractions of N_2 and O_2 are 0,79 and 0,21 respectively.

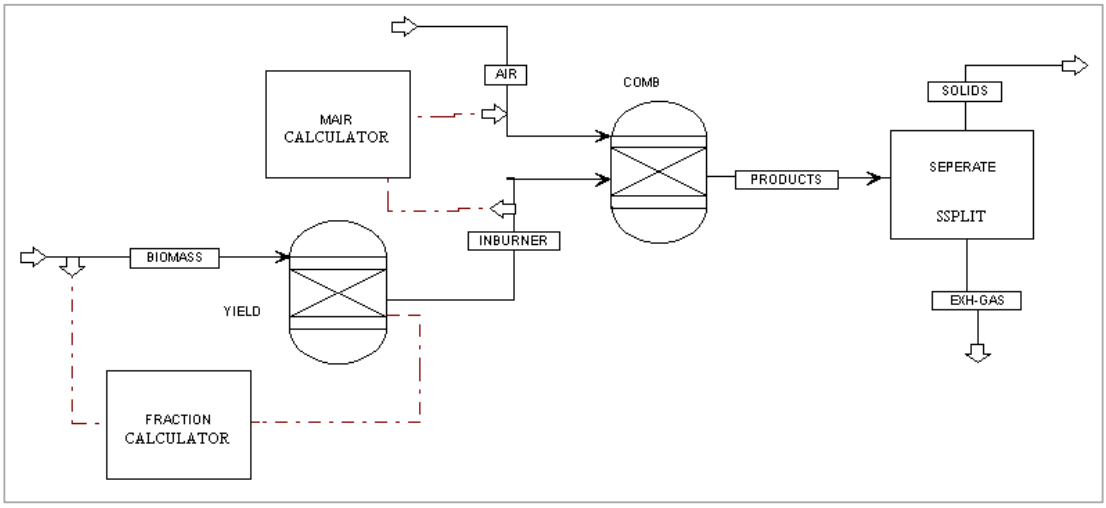

Figure 39 Block Diagram of Biomass Combustion Process

“RGibbs” block (“COMB” in Figure 39) is used to model reactions that come to thermal equilibrium. “COMB” calculates chemical equilibrium and phase equilibrium by minimizing the Gibbs free energy of the system. Biomass should be decomposed into its components so that they can be the input to the “COMB” where the combustion takes place.

“RYield” block (“YIELD”) decomposes biomass into specified components. Components consist of H_2O, C (solid), ash, H_2, N_2, O_2, CL_2 and S. “Calculator” block

(“FRACTION”) is utilized to calculate the yields based on component attributes of the biomass. “FRACTION” uses the data keyed in ultanal and proxanal attributes. However, the data is dry basis and to be able to calculate actual yields it should be converted into wet basis data. The moisture content is known, so the formula which converts the dry basis values into wet basis can be written in “FRACTION”. The outlet stream of “YIELD” is named as “INBURNER” and represents the decomposed biomass material.

“INBURNER” and “AIR” are fed into “COMB” where they are mixed and burnt. Possible products are identified as H_2O, N_2, O_2, NO_2, NO, H_2, C (pure solid), CO, CO_2. Combustion products are indicated by “PRODUCT” stream. “SSPLIT” block (“SEPARATE”) is utilized to separate the solid and gas particles formed after combustion. Separation is done according to the sub-stream properties and two outlet streams is formed. “EXH-GAS”, exhaust gases, stands for the products in gaseous phase whereas “SOLIDS” represents the solid products such as ash. Split fraction value for “MIXED” sub-stream of “EXH-GAS” should be entered as 1.

Exhaust gas is fed through series of “HEATER” blocks which symbolize the economizer, evaporator and super-heater parts of the biomass boiler shown in Figure 40.

As it is explained for the heat exchanger in Solar Field, two “HEATER” blocks with a heat stream connecting them is used to simulate heat exchangers in ASPEN PLUS. Biomass boiler has three stages and “1”, “2” & “3” are the heat streams representing the heat transfer for each stage from the exhaust gas to the water. “THWAT-IN” is the water stream which enters the boiler at 40 bar and 25 °C (ambient temperature). “ECON” stands for the economizer where the inlet water is heated up to its boiling point at constant pressure. In the “specifications” window, pressure should be set to 0 bar and vapor fraction should be indicated as 0,001. “EVAP” symbolizes the evaporator in which the water is heated further and phase change occurs. Vapor fraction in that block should be set as 1, meaning that all of the water evaporates and the exit stream is at gas phase.

“SPHEATER” represents the super-heater section and specifications of “SPHEATER” are different for each case. For CASE-1 (with auxiliary boiler) temperature of the block is set as the turbine inlet temperature (540°C) and 0 bar is inputted as the pressure value. In CASE-2 (where the vapor coming from the solar field is mixed with the vapor coming from the super-heater), temperature of the exit stream of super-heater is manipulated by a “Design-Spec” block (“TEMP-VAP” in Figure 41) to obtain 540°C mixture temperature.

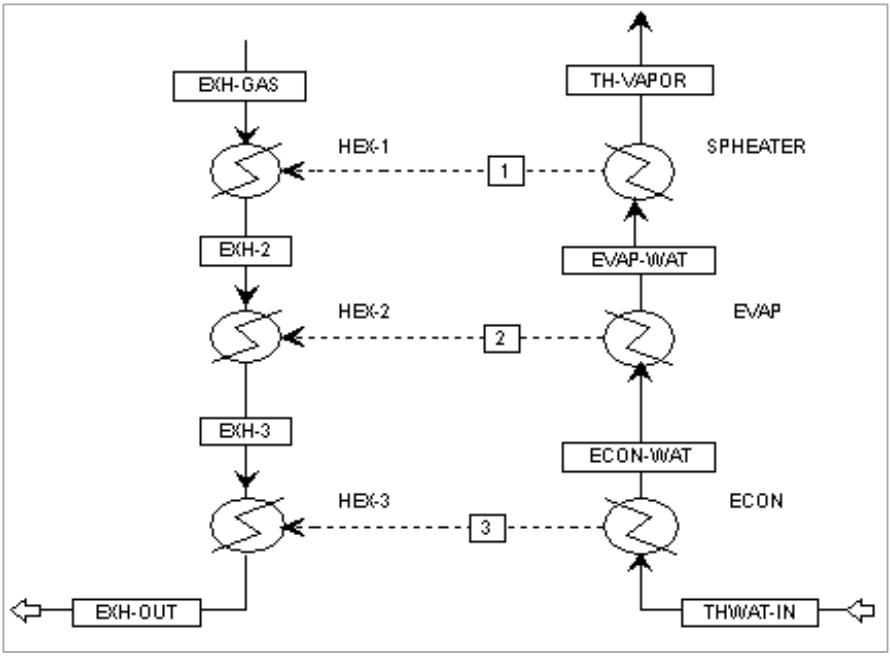

Figure 40 Block Diagram of Biomass Boiler

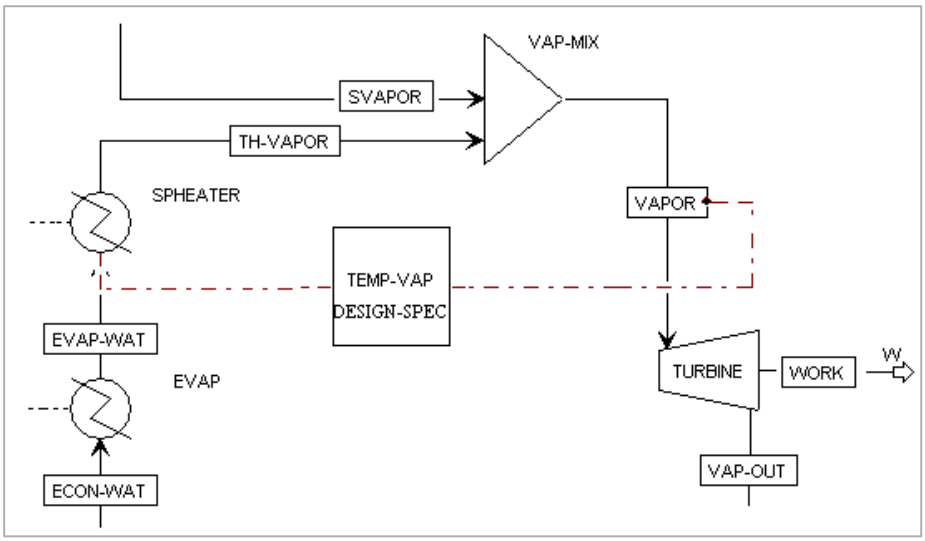

Figure 41 Block Diagram of Super-Heater of Biomass Boiler (CASE-2)

3) Steam Turbine

"VAPOR" refers to the incoming steam at 530ºC, 40 bar. "COMPR" block (TURBINE) with "turbine" option is used to simulate the steam turbine. Isentropic and mechanical efficiencies of the turbine is taken as 85% and 98% respectively. "VAP-OUT" represents the vapor leaving the turbine at 0.1 bar. Pressure ratio of the steam turbine is 400. "WORK" stands for work output of turbine.

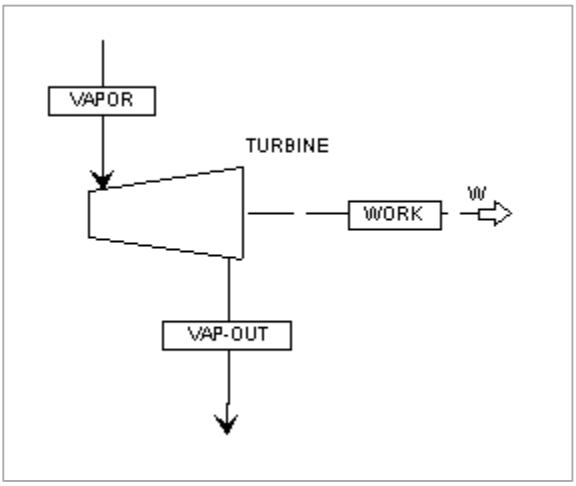

Figure 42 Block Diagram of Steam Turbine

4) Condenser

Simulation of the condenser is developed by using a "HEATER" block ("CONDENSE). Figure 43 shows the block diagram of condenser.

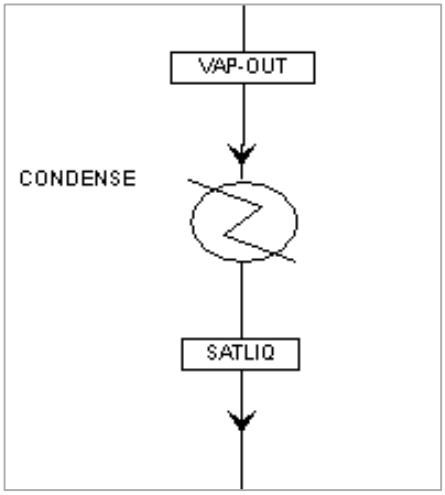

Figure 43 Block Diagram of Condenser

Phase change occurs in condenser and the water at saturated liquid phase at 0.1 bar leaves the condenser ("SATLIQ").

5) Pump

"PUMP" block ("PUMP") is used for the simulation of pump. Pump increases the pressure of saturated liquid from 0.1 bar to boiler pressure (40 bar). Isentropic efficiency of the pump is taken as 85%. "WATER" refers to the pressurized water leaving the pump.

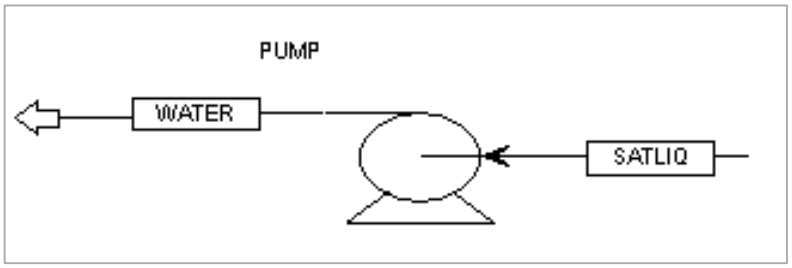

Figure 44 Block Diagram of Pump

6) Auxiliary Boiler

Figure 45 shows the block diagram of auxiliary boiler. Auxiliary boiler is indicated by a "HIERARCHY" block ("AUX-BOIL") in which combustion of methane and superheating of steam take place. "RGIBBS" reactor is used to simulate the combustion of methane. Two "HEATER" blocks are considered to represent the heat exchange process between exhaust gas and steam.

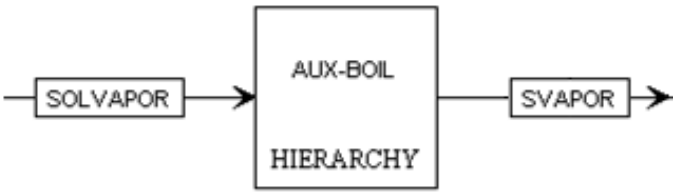

Figure 45 Block Diagram of Auxiliary Boiler

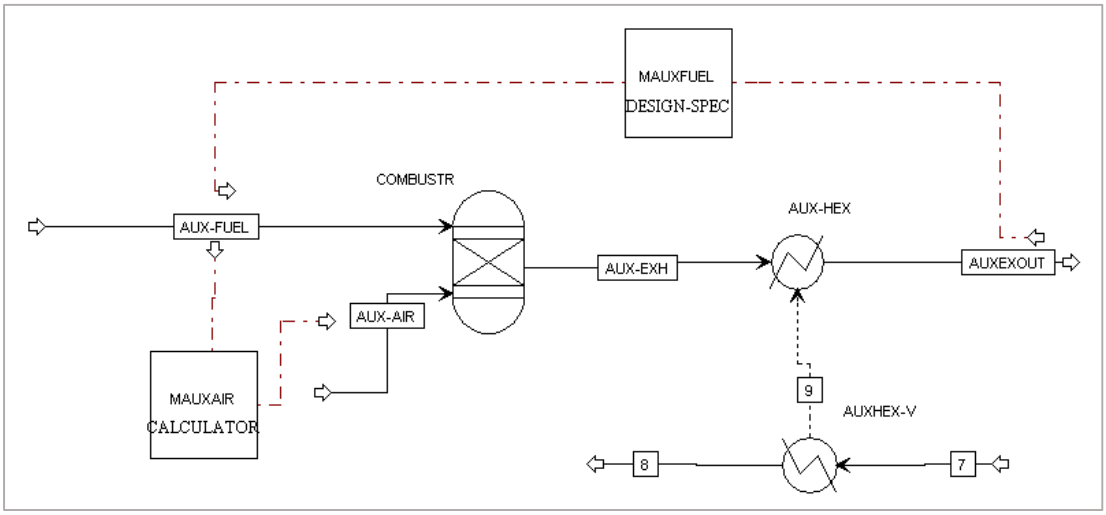

Figure 46 Block Diagram of Auxiliary Boiler (content of HIERARCHY Block)

APPENDIX B

Table B-1: Kırklareli DNI Values (monthly)

Hour	Jan.	Feb.	Mar.	Apr.	May	Jun.
1	0,0	0,0	0,0	0,0	0,0	0,0
2	0,0	0,0	0,0	0,0	0,0	0,0
3	0,0	0,0	0,0	0,0	0,4	2,8
4	0,0	0,0	0,0	6,7	33,9	79,6
5	0,0	1,3	18,5	100,3	170,4	291,7
6	5,5	26,7	154,7	250,9	301,7	444,3
7	127,8	161,8	303,9	355,2	370,1	550,9
8	299,2	250,9	375,1	441,0	481,4	592,4
9	379,7	257,6	419,3	487,2	526,0	586,7
10	407,7	327,4	428,1	485,2	461,1	556,4
11	390,2	297,9	390,6	458,7	474,4	500,6
12	365,7	306,6	378,2	424,9	454,2	475,2
13	337,2	254,7	387,4	391,8	437,8	445,7
14	191,2	199,0	343,9	348,7	361,5	405,5
15	46,0	125,1	250,7	303,8	320,8	426,3
16	0,7	14,9	110,2	217,8	284,2	374,1
17	0,0	0,0	2,9	36,2	122,4	249,4
18	0,0	0,0	0,0	0,0	4,1	19,0
19	0,0	0,0	0,0	0,0	0,0	0,0
20	0,0	0,0	0,0	0,0	0,0	0,0
21	0,0	0,0	0,0	0,0	0,0	0,0
22	0,0	0,0	0,0	0,0	0,0	0,0
23	0,0	0,0	0,0	0,0	0,0	0,0
24	0,0	0,0	0,0	0,0	0,0	0,0

Table B-1: Kırklareli DNI Values (monthly) (continued)

Hour	July	Aug.	Sep.	Oct.	Nov.	Dec.
1	0,0	0,0	0,0	0,0	0,0	0,0
2	0,0	0,0	0,0	0,0	0,0	0,0
3	0,5	0,0	0,0	0,0	0,0	0,0
4	42,1	14,6	0,9	0,0	0,0	0,0
5	230,1	232,5	134,3	17,2	0,1	0,0
6	401,9	496,9	428,8	256,7	38,9	5,6
7	517,7	644,5	563,3	468,2	157,8	59,0
8	577,6	698,6	642,1	551,3	233,9	128,7
9	599,3	675,9	671,6	599,3	269,1	164,0
10	615,0	684,8	668,3	578,8	285,0	192,8
11	581,8	672,8	622,0	536,6	276,3	196,0
12	506,5	661,9	587,6	443,6	246,9	165,9
13	455,8	627,6	565,3	367,0	157,0	116,6
14	428,8	608,3	520,7	355,0	112,9	50,8
15	416,6	497,4	408,7	194,4	21,5	9,5
16	346,3	390,3	180,0	14,1	0,0	0,0
17	214,8	133,2	6,6	0,0	0,0	0,0
18	13,7	1,9	0,0	0,0	0,0	0,0
19	0,0	0,0	0,0	0,0	0,0	0,0
20	0,0	0,0	0,0	0,0	0,0	0,0
21	0,0	0,0	0,0	0,0	0,0	0,0
22	0,0	0,0	0,0	0,0	0,0	0,0
23	0,0	0,0	0,0	0,0	0,0	0,0
24	0,0	0,0	0,0	0,0	0,0	0,0